

Secure Transmission for Hierarchical Information Accessibility in Downlink MU-MIMO

Kanguk Lee, Jinseok Choi, Dong Ku Kim, and Jeonghun Park

Abstract

Physical layer security is a useful tool to prevent confidential information from wiretapping. In this paper, we consider a generalized model of conventional physical layer security, referred to as hierarchical information accessibility (HIA). A main feature of the HIA model is that a network has a hierarchy in information accessibility, wherein decoding feasibility is determined by a priority of users. Under this HIA model, we formulate a sum secrecy rate maximization problem with regard to precoding vectors. This problem is challenging since multiple non-smooth functions are involved into the secrecy rate to fulfill the HIA conditions and also the problem is non-convex. To address the challenges, we approximate the minimum function by using the LogSumExp technique, thereafter obtain the first-order optimality condition. One key observation is that the derived condition is cast as a functional eigenvalue problem, where the eigenvalue is equivalent to the approximated objective function of the formulated problem. Accordingly, we show that finding a principal eigenvector is equivalent to finding a local optimal solution. To this end, we develop a novel method called generalized power iteration for HIA (GPI-HIA). Simulations demonstrate that the GPI-HIA significantly outperforms other baseline methods in terms of the secrecy rate.

I. INTRODUCTION

As the amount of information delivered through a wireless medium rapidly increases, security in wireless communications becomes a critical issue to prevent leakage of confidential

K. Lee and J. Park are with the School of Electronics Engineering, College of IT Engineering, Kyungpook National University, Daegu, 41566, South Korea (e-mail: kanguk.lee@knu.ac.kr and jeonghun.park@knu.ac.kr). J. Choi is with Department of Electrical Engineering, Ulsan National Institute of Science and Technology, South Korea (e-mail: jinseokchoi@unist.ac.kr). D. Kim is with Department of Electrical and Electronic Engineering, Yonsei University, South Korea (e-mail: dkkim@yonsei.ac.kr)

This work was supported by the National Research Foundation of Korea (NRF) grant funded by the Korea government (MSIT) (No. 2019R1G1A1094703) and (No. 2021R1C1C1004438).

A part of this paper will be presented in IEEE Globecom 2021 [1].

information. Due to the broadcast nature of a wireless medium, it is challenging to implement a secure communication system. Considering a cellular network, for example, if an eavesdropper is located within a coverage region, it is not possible to physically prevent the eavesdropper from overhearing the signals transmitted from a base station (BS). Classical approaches to protect the information from eavesdropping rely on cryptography [2]. Unfortunately, it requires high implementation costs caused by the key distribution and complicated encryption algorithms. As a complement, physical layer security [3] has been gaining attention.

From an information theoretical point-of-view, physical layer security shows that a transmitter can reliably send a confidential message to legitimate users with a positive rate, ensuring that an eavesdropper is not able to decode it provided that the eavesdroppers' channel quality is no better than that of the legitimate users' channel. This non-zero transmission rate is referred to as *the secrecy rate*. One underlying assumption of physical layer security so far is that two classes of receivers exist in a network: legitimate users and malignant eavesdroppers. Nevertheless, this traditional binary security configuration is limited in that it is infeasible to reflect a complicated security structure that will be used in 6G. Specifically, as applications of wireless communications have become diversified, a network can have a hierarchy in information access [4], so that even some legitimate users can be prohibited to decode particular messages depending on their security clearances.

Motivated by this, [5] presented a new model that generalizes physical layer security by incorporating a hierarchical security structure. In this model, each user is assigned into a layer whose priority is different, and the decoding feasibility is determined by the layer. For example, users in a higher security level layer are permitted to decode a message intended to lower security level layers, while the opposite direction access is prohibited. We refer this model as hierarchical information accessibility (HIA). The HIA model is useful since it is a generalization of a conventional physical layer security model. Specifically, assuming that only two layers exist and a transmitter only delivers a message to one of the two layers, the corresponding HIA model is reduced to a conventional physical layer security setup that assumes legitimate users and illegal eavesdroppers. An efficient secure transmission method for the HIA, however, has not been known yet. Although [5] investigated a transmit power minimization problem, a general secure transmission solution to maximize the sum secrecy rate for the HIA is missing. In this paper, we aim to fill this missing block by proposing a novel method.

A. Prior Works

There have been several prior works that developed secure precoding solutions to maximize the secrecy rate. Focusing on a multi-user setup considered in this paper, a strategy to exploit the multi-user interference in a beneficial way to degrade eavesdropper's channel quality was developed in [6]. In [7], a sum secrecy rate optimization problem was formulated and a successive convex approximation technique was presented to relax the problem. In [8], assuming a wireless network that consists of multiple transmitter-receiver pairs and one eavesdropper, algorithms to maximize the secrecy rate and the secrecy energy efficiency were presented. Extending [8], considering multiple eavesdroppers, [9] proposed a secure transmission algorithm to maximize the sum secrecy rate. In [10], when multiple eavesdroppers collude to decode confidential messages, an optimization framework to maximize the sum secrecy rate was proposed. In [11], [12], secure antenna selection methods were investigated.

In common, the aforementioned prior works considered conventional physical layer security, wherein two classes of receivers exist. Assuming the generalized HIA model, in [5], a precoding design to minimize the transmit power was developed under quality of service constraints. In [13], a non-orthogonal multiple access (NOMA) scheme with multicast-unicast messages was considered. In this scenario, a power allocation with successive interference cancellation (SIC) was developed to enhance the security performance. Similar to this, a secure transmission with NOMA was also studied in [14]. What is missing in the literature is a general precoding solution that maximizes the sum secrecy rate in the HIA; yet such a solution is necessary to reap de facto performance gains from the HIA model. Finding such a solution, however, is particularly difficult since a sum secrecy rate maximization problem is non-convex, where finding a global optimum solution is infeasible. Even worse, to guarantee the HIA condition, the multiple minimum (or maximum) functions are complicatedly intertwined into the secrecy information rate, which makes the problem harder to solve.

B. Contributions

In this paper, we put forth a secure precoding method to maximize the sum secrecy rate of HIA systems. We consider a single-cell downlink system, where a multiple-antenna base station (BS) serves multiple single-antenna users. In this system, the HIA is considered, wherein the users are assigned to a particular layer whose security level is different. It is required to ensure that the users in the higher layer are able to decode the messages intended to the lower layers, while

the users in the lower layer cannot decode messages intended to the higher layers. Assuming K layers, the BS sends K independent messages, where the same message is intended to the users in the same layer, i.e., multi-group multicast message scenario [15], [16]. In such a setup, our main contributions are summarized as follows:

- To accomplish the HIA condition, we adopt a notion of physical layer security. The secrecy rate of the message for layer k is determined by the minimum value of the rates that can be achieved at the users in the higher layers ($\geq k$, to guarantee that the higher layer users can decode it), subtracted by the wiretapping lower layer users' rates ($< k$, to guarantee that the lower layer users cannot decode it). The wiretapping lower layer users' rate is determined differently depending on whether the lower layer users collude or not. Assuming the non-colluding case, the wiretapping channel's rate is determined by the maximum value of the rates that can be achieved at users in the lower layers. In the colluding case, the effective SINR of the wiretapping channel's rate is the sum of the SINR of each lower layer user.
- Considering each non-colluding and colluding case, we characterize the achievable secrecy rates. Leveraging this, we formulate optimization problems to maximize the sum secrecy rate with regard to precoding vectors. Unfortunately, the formulated problems are challenging to solve since the multiple non-smooth minimum and maximum functions are complicatedly involved into the secrecy rate and the problems are non-convex. To resolve this, we first approximate our problem using the LogSumExp technique that makes the problem smooth. Then, we reformulate the problem as a form of Rayleigh quotients by rewriting the optimization variables onto a higher dimensional vector. With this form, we derive the first-order optimality condition and show that the derived optimality condition is cast as a functional eigenvalue problem. One remarkable point is that the corresponding matrix is a function of the eigenvector itself, and the eigenvalue is equivalent with the approximated objective function. Accordingly, finding the principal eigenvector is equivalent to finding the local optimal point that has zero gradient. Based on this insight, we propose an algorithm inspired by power iteration, referred as generalized power iteration for HIA (GPI-HIA) that finds the principal eigenvector of the derived functional eigenvalue problems.
- In the HIA model, due to the hierarchy of the information access, sequential decoding with SIC is a natural choice at the high layer users, which makes similarity between HIA and downlink NOMA systems. We show that the main problem to maximize the sum secrecy

rate in the HIA model can be reduced to a sum rate maximization problem in typical downlink NOMA systems with a fixed decoding order. Specifically, by assuming that only one user is included in each layer and ignoring security to protect the higher layer message from the lower layer users, our HIA model becomes equivalent to downlink multi-antenna NOMA. Leveraging this, we also propose a sum rate maximization precoding method for downlink NOMA with a fixed decoding order.

- In numerical results, we validate the performance of the proposed GPI-HIA. Thanks to the fact that the GPI-HIA properly incorporates the complicated rate conditions into its optimization process, it achieves more than 400% secrecy rate gains over an existing convex relaxation based precoding method. Further, we also show that a fairness issue caused by an imbalance between the layers is resolved by modifying the proposed method. Additionally, we present that the proposed precoding method for downlink NOMA also provides considerable rate gains. In addition to those performance benefits, the proposed method does not require any off-the-shelf optimization solver such as CVX. In this sense, our method is beneficial not only in a performance perspective, but also in an implementation perspective.

Notation: the superscripts $(\cdot)^T$, $(\cdot)^H$, and $(\cdot)^{-1}$ denote the transpose, Hermitian, and matrix inversion, respectively. $\|\cdot\|_F$ and $\|\cdot\|$ denote the Frobenious norm and the ℓ_2 norm. \mathbf{I}_N is the identity matrix with size $N \times N$. Assuming that $\mathbf{A}_1, \dots, \mathbf{A}_K \in \mathbb{C}^{N \times N}$, $\mathbf{A} = \text{blkdiag}(\mathbf{A}_1, \dots, \mathbf{A}_k, \dots, \mathbf{A}_K) \in \mathbb{C}^{NK \times NK}$ is a block diagonal matrix.

II. SYSTEM MODEL

A. Hierarchical Information Accessibility

We consider a single-cell downlink MIMO network, where a BS equipped with N antennas serves M single antenna users. In our HIA model, there exist K layers, where each layer includes a subset of the users. Denoting the user set as $\mathcal{M} = \{1, \dots, M\}$ and the k -th layer as \mathcal{L}_k for $k \in \{1, \dots, K\}$, all the users are assigned to a specific layer, i.e., $\mathcal{M} = \bigcup_{k=1}^K \mathcal{L}_k$ and each user is not allocated to more than one layer, i.e., $\mathcal{L}_i \cap \mathcal{L}_j = \emptyset$, $i \neq j$. The users in the same layer receive the same message, which corresponds to a multi-group multicast message scenario [15], [16]. For instance, the BS transmits the message s_k to the users in \mathcal{L}_k .

In the considered HIA model, the users assigned to different layers have different security priorities that determine information accessibility. This priority is indicated by the index of the

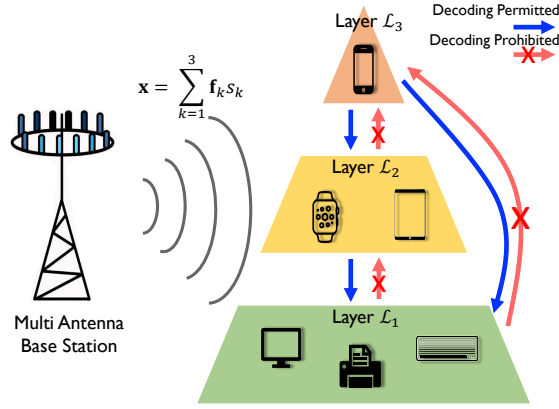


Fig. 1. Generalized illustration of the considered HIA when $K = 3$, $|\mathcal{L}_1| = 3$, $|\mathcal{L}_2| = 2$ and $|\mathcal{L}_3| = 1$.

layer. For example, if $i > j$, the users in \mathcal{L}_i have higher priority than the users in \mathcal{L}_j . In the HIA, the users with the higher priority are able to access the lower priority information, i.e., the users in \mathcal{L}_i can decode the message s_j for $i \geq j$. On the contrary, the users with the lower priority are prohibited to access the information intended the higher priority users. That is to say, the users in \mathcal{L}_j should not decode the message s_i for $i > j$. From a viewpoint of the physical layer security, the users assigned to the lower priority layer are treated as eavesdroppers to the users in the higher priority layer.

We illustrate an example of the considered HIA system model in Fig. 1. As observed in the figure, the users in the higher priority layer, i.e., \mathcal{L}_3 , are permitted to decode the message delivered to the lower priority layers, i.e., \mathcal{L}_1 and \mathcal{L}_2 . On the contrary to that, the users in the lower priority layers are prohibited to decode the message with higher priority.

B. Channel Model

We denote the channel vector from the BS to the i -th user included in \mathcal{L}_ℓ as $\mathbf{h}_{i,\ell} \in \mathbb{C}^{N \times 1}$ for $i \in \mathcal{L}_\ell$. This channel vector follows the correlated Gaussian distribution, i.e., $\mathbf{h}_{i,\ell} \sim \mathcal{CN}(\mathbf{0}, \mathbf{R}_{i,\ell})$ where $\mathbf{R}_{i,\ell} = \mathbb{E}[\mathbf{h}_{i,\ell} \mathbf{h}_{i,\ell}^H] \in \mathbb{C}^{N \times N}$ is the channel covariance matrix. The channel covariance matrix is constructed according to the geometric one-ring scattering model [17]. Specifically, assuming that the BS is equipped with uniform circular array of N isotropic antennas and radius λD where λ is wavelength and $D = \frac{0.5}{\sqrt{(1 - \cos(2\pi/N))^2 + \sin(2\pi/N)^2}}$, the channel correlation coefficient between n -th antenna and m -th antenna of $\mathbf{R}_{i,\ell}$ is obtained as

$$[\mathbf{R}_{i,\ell}]_{n,m} = \frac{\beta_{i,\ell}}{2\Delta_{i,\ell}} \int_{\theta_{i,\ell} - \Delta_{i,\ell}}^{\theta_{i,\ell} + \Delta_{i,\ell}} e^{-j \frac{2\pi}{\lambda} \Psi(x)(\mathbf{r}_n - \mathbf{r}_m)} dx, \quad (1)$$

where $\beta_{i,\ell}$ is a large scale fading, $\Delta_{i,\ell}$ is a angular spread, $\theta_{i,\ell} \in [0, 2\pi]$ is an angle-of-arrival (AoA), $\Psi(x) = [\cos(x), \sin(x)]$ is a wave vector for a planar wave colliding with the angular x , and \mathbf{r}_n is a position vector of n -th antenna of BS. By employing the Karhunen-Loeve model as in [17], [18], the channel vector $\mathbf{h}_{i,\ell}$ is characterized as $\mathbf{h}_{i,\ell} = \mathbf{U}_{i,\ell} \mathbf{\Lambda}_{i,\ell}^{\frac{1}{2}} \mathbf{g}_{i,\ell}$, where $\mathbf{U}_{i,\ell}$ contains the eigenvectors of $\mathbf{R}_{i,\ell}$, $\mathbf{\Lambda}_{i,\ell}$ is a diagonal matrix whose elements are non-zero eigenvalues of $\mathbf{R}_{i,\ell}$, and $\mathbf{g}_{i,\ell}$ is an independent and identically distributed channel vector drawn from $\mathcal{CN}(\mathbf{0}, \mathbf{I})$. Further, we consider a block fading channel, so that $\mathbf{g}_{i,\ell}$ is invariant during a channel coherence time. In this paper, we assume that the BS knows the perfect CSIT.

C. Signal Model

As the multi-group multicast scenario is assumed, K independent messages are transmitted from the BS [15], [16]. Using linear precoding, the transmit signal $\mathbf{x} \in \mathbb{C}^{N \times 1}$ is represented as

$$\mathbf{x} = \sum_{k=1}^K \mathbf{f}_k s_k, \quad (2)$$

with the power constraint $\sum_{k=1}^K \|\mathbf{f}_k\|^2 = 1$ where \mathbf{f}_k is a $N \times 1$ precoding vector for s_k .

Now we explain the decoding process in the HIA model. Recalling that the users in the higher priority can decode the messages sent to the lower priority layers, we assume that the decoding at each user proceeds sequentially from messages sent to the lowest layer to the highest layer, i.e., $1 \rightarrow K$. With this sequential decoding architecture, SIC is inherently exploited to eliminate the lower layer messages after decoding them. Using SIC, when the user in \mathcal{L}_ℓ attempts to decode s_k where $k \leq \ell$, the interference only comes from the messages intended to the layer $\mathcal{L}_{k+1}, \dots, \mathcal{L}_K$. For example, letting $K = 3$, the user in \mathcal{L}_3 has an access to the messages s_1, s_2 , and s_3 . This user first attempts to decode s_1 , while treating s_2 and s_3 as interference. Once the user succeeds to decode s_1 , the user eliminates s_1 from the received signal and decodes s_2 with the reduced amount of the interference. After cancelling s_2 , the user finally decodes s_3 .

Considering the SIC decoding process for the HIA model, the signal model of the user i in \mathcal{L}_ℓ when decoding s_k is written as

$$y_{k,i,\ell} = \underbrace{\mathbf{h}_{i,\ell}^H \mathbf{f}_k s_k}_{\text{desired signal}} + \underbrace{\sum_{j=k+1}^K \mathbf{h}_{i,\ell}^H \mathbf{f}_j s_j}_{\text{interference}} + n_{i,\ell}, \quad (3)$$

where $n_{i,k} \sim \mathcal{CN}(0, \sigma^2)$ is additive white Gaussian noise. As explained above, we observe that the interference only comes from the higher layer messages, i.e., $k+1, \dots, K$. Assuming that s_k

is drawn from a Gaussian distribution, i.e., $\mathcal{CN}(0, P)$ where P is symbol power, the achievable rate of the message s_k at the user i in \mathcal{L}_ℓ is determined as

$$R_{k,i,\ell} = \log_2 \left(1 + \frac{|\mathbf{h}_{i,\ell}^H \mathbf{f}_k|^2}{\sum_{j=k+1}^K |\mathbf{h}_{i,\ell}^H \mathbf{f}_j|^2 + \frac{\sigma^2}{P}} \right). \quad (4)$$

D. Performance Metrics and Problem Formulation

In this subsection, we characterize the secrecy rate for the HIA model and formulate main problems. To prevent the low priority users from decoding the high priority messages, we adopt a notion of physical layer security. From a perspective of the high priority message, the low priority users behave as eavesdroppers. Using physical layer security, by appropriately determining the secrecy rate as a function of the SINR of the low priority users, secure transmission is accomplished. The secrecy rate is determined in a different way depending on whether the low priority users collude or not. In the following, we characterize the secrecy rate considering the non-colluding and the colluding case respectively.

To simplify the secrecy rate performance characterization, we assume the worst case [19], [20], where the eavesdroppers (low priority users) in $\mathcal{L}_{\ell'}$ already remove the messages s_j when attempting to decode the message s_k , $\ell' < j < k$. We note that this assumption results in a lower bound performance as it increases the eavesdropper's SINR.

1) *Non-Colluding Case:* first, we consider the non-colluding case. In this case, we assume that the low priority users do not cooperate to decode the high priority message. Then, the secrecy rate for s_k is obtained as

$$\bar{R}_k^{\text{nc}} = \left[\min_{i \in \mathcal{L}_\ell, \ell \geq k} R_{k,i,\ell} - \max_{i' \in \mathcal{L}_{\ell'}, \ell' < k} R_{k,i',\ell'} \right]^+. \quad (5)$$

The first term at the right-hand side (r.h.s.) of (5) is the minimum rate among the users allowed to decode s_k . This is for ensuring that all the users in the layers $\ell \geq k$ are able to decode s_k . The second term at the r.h.s. of (5) is the maximum rate among the wiretapping users, i.e., the users in the layers that has no right to decode s_k . This is because, in the presence of multiple non-colluding eavesdroppers, no eavesdropper can decode a message when the strongest eavesdropper cannot decode it [9], [12], [21]. For this reason, the required redundancy to protect s_k is determined by the maximum rate among all the eavesdroppers, i.e., the users in the layers $\ell' < k$. Consequently, in the non-colluding case, the HIA condition is fulfilled when the information rate of s_k is set as \bar{R}_k^{nc} in (5).

Now, we aim to maximize the sum secrecy rate with respect to the precoding vectors. Accordingly, the optimization in the non-colluding case is formulated as

$$\max_{\mathbf{f}_1, \dots, \mathbf{f}_K} \sum_{k=1}^K \bar{R}_k^{\text{nc}} \quad (6)$$

$$\text{subject to } \sum_{k=1}^K \|\mathbf{f}_k\|^2 = 1. \quad (7)$$

Unfortunately, it is infeasible to directly solve (6) because of two main difficulties: *i*) (6) is non-convex, wherein finding a global optimal solution is infeasible, *ii*) for the HIA condition, the rate of each message is determined in a complicatedly intertwined way, including the multiple minimum functions.

2) *Colluding Case*: next, we consider the colluding case; we assume that the low priority users cooperate to jointly decode the high priority messages. Then, the wiretapping channels form a virtual multiple receive antenna channel, so that the effective SINR is the sum of individual SINR of each eavesdropper [10]. Accordingly, the secrecy rate for s_k is characterized as

$$\bar{R}_k^{\text{c}} = \left[\min_{i \in \mathcal{L}_\ell, \ell \geq k} R_{k,i,\ell} - R_{k,i',\ell'}^{\text{e}} \right]^+, \quad (8)$$

where

$$R_{k,i',\ell'}^{\text{e}} = \log_2 \left(1 + \sum_{\ell'=1}^{k-1} \sum_{i' \in \mathcal{L}_{\ell'}} \frac{|\mathbf{h}_{i',\ell'}^{\text{H}} \mathbf{f}_k|^2}{\sum_{j=k+1}^K |\mathbf{h}_{i',\ell'}^{\text{H}} \mathbf{f}_j|^2 + \frac{\sigma^2}{P}} \right). \quad (9)$$

We note that the difference of (8) from (5) is the second term at the r.h.s., i.e., the achievable rate of the wiretapping channel. In the colluding case, the HIA condition is satisfied provided that the information rate of s_k is set as \bar{R}_k^{c} in (8).

As in the non-colluding case, we aim to maximize the sum secrecy rate with respect to the precoding vectors by solving the following problem:

$$\max_{\mathbf{f}_1, \dots, \mathbf{f}_K} \sum_{k=1}^K \bar{R}_k^{\text{c}} \quad (10)$$

$$\text{subject to } \sum_{k=1}^K \|\mathbf{f}_k\|^2 = 1. \quad (11)$$

Similar to the non-colluding case, it is infeasible to directly solve (10) due to its non-convexity and non-smoothness.

In the next sections, we put forth the proposed methods to find a local optimal solution of (6) and (10) by resolving the challenges.

Remark 1 (HIA as a generalized model). The presented HIA model generalizes conventional physical layer security. For instance, assuming that $K = 2$ and $\mathbf{f}_1 = \mathbf{0}$, the users included in \mathcal{L}_1 are eavesdroppers attempting to overhear s_2 and the users in \mathcal{L}_2 are legitimate users receiving multicast message s_2 . This is equivalent to conventional physical layer security with a multicast message setup [22].

In addition to that, the HIA model also can be reduced to a downlink NOMA scenario. For instance, we assume that a single-user is included in each layer, i.e., $|\mathcal{L}_k| = 1$ and ignore security, i.e., we do not care lower layer users to overhear higher layer messages. Then, the optimization problem (6) reduces to a sum rate maximization problem of downlink NOMA, whose decoding order is fixed as $1 \rightarrow K$ [23]. Accordingly, our method to solve (6) is also useful in downlink NOMA. We explain this in detail later.

III. PRECODING OPTIMIZATION IN THE NON-COLLUDING CASE

We explain the ideas to solve the optimization problems (6) in the non-colluding case. First, to convert the problem into a tractable form, we approximate the minimum and maximum functions involved in (6) using the LogSumExp technique. Subsequently, we represent the approximated objective function as a form of Rayleigh quotients by rewriting the precoding vector onto a higher dimensional vector. With this form, we derive the first-order optimality condition and put forth an efficient algorithm to find the principal eigenvector exploiting our novel interpretation of the derived optimality condition through a lens of a functional eigenvalue problem.

A. Reformulation to a Tractable Form

First, we approximate the non-smooth minimum function by using the LogSumExp technique. With the technique, the minimum and maximum functions are approximated as [24], [25]

$$\min_{i=1,\dots,N} \{x_i\} \approx -\frac{1}{\alpha} \log \left(\sum_{i=1}^N \exp(-x_i \alpha) \right), \quad (12)$$

$$\max_{i=1,\dots,N} \{x_i\} \approx \frac{1}{\alpha} \log \left(\sum_{i=1}^N \exp(x_i \alpha) \right), \quad (13)$$

where the approximation becomes tight as $\alpha \rightarrow \infty$. Leveraging (12) and (13), we obtain the following approximations

$$\min_{i \in \mathcal{L}_\ell, \ell \geq k} R_{k,i,\ell} \approx -\frac{1}{\alpha} \log \left(\sum_{\ell=k}^K \sum_{i \in \mathcal{L}_\ell} e^{-\alpha R_{k,i,\ell}} \right), \quad (14)$$

$$\max_{i' \in \mathcal{L}_{\ell'}, \ell' < k} R_{k,i',\ell'} \approx \frac{1}{\alpha} \log \left(\sum_{\ell'=1}^{k-1} \sum_{i' \in \mathcal{L}_{\ell'}} e^{\alpha R_{k,i',\ell'}} \right). \quad (15)$$

Next, we define a higher dimensional precoding vector $\bar{\mathbf{f}}$ by stacking the original precoding vectors $\mathbf{f}_1, \dots, \mathbf{f}_K$. Accordingly, $\bar{\mathbf{f}}$ is given by

$$\bar{\mathbf{f}} = [\mathbf{f}_1^\top, \dots, \mathbf{f}_K^\top]^\top \in \mathbb{C}^{NK \times 1}. \quad (16)$$

With (16), we rewrite the (4) as

$$\begin{aligned} R_{k,i,\ell} &= \log_2 \left(1 + \frac{|\mathbf{h}_{i,\ell}^\mathbf{H} \mathbf{f}_k|^2}{\sum_{j=k+1}^K |\mathbf{h}_{i,\ell}^\mathbf{H} \mathbf{f}_j|^2 + \frac{\sigma^2}{P}} \right) = \log_2 \left(\frac{\sum_{j=k}^K \mathbf{f}_j^\mathbf{H} \mathbf{h}_{i,\ell} \mathbf{h}_{i,\ell}^\mathbf{H} \mathbf{f}_j + \frac{\sigma^2}{P}}{\sum_{j=k+1}^K \mathbf{f}_j^\mathbf{H} \mathbf{h}_{i,\ell} \mathbf{h}_{i,\ell}^\mathbf{H} \mathbf{f}_j + \frac{\sigma^2}{P}} \right) \\ &= \log_2 \left(\frac{\bar{\mathbf{f}}^\mathbf{H} \mathbf{A}_{k,i,\ell} \bar{\mathbf{f}}}{\bar{\mathbf{f}}^\mathbf{H} \mathbf{B}_{k,i,\ell} \bar{\mathbf{f}}} \right), \end{aligned} \quad (17)$$

where

$$\mathbf{A}_{k,i,\ell} = \text{blkdiag} \left(\mathbf{0}, \dots, \mathbf{0}, \underbrace{\mathbf{h}_{i,\ell} \mathbf{h}_{i,\ell}^\mathbf{H}}_{k\text{th block}}, \dots, \mathbf{h}_{i,\ell} \mathbf{h}_{i,\ell}^\mathbf{H} \right) + \frac{\sigma^2}{P} \mathbf{I}_{NK} \in \mathbb{C}^{NK \times NK}, \quad (18)$$

$$\mathbf{B}_{k,i,\ell} = \mathbf{A}_{k,i,\ell} - \text{blkdiag} \left(\mathbf{0}, \dots, \mathbf{0}, \underbrace{\mathbf{h}_{i,\ell} \mathbf{h}_{i,\ell}^\mathbf{H}}_{k\text{th block}}, \mathbf{0}, \dots, \mathbf{0} \right) \in \mathbb{C}^{NK \times NK}. \quad (19)$$

Subsequently, leveraging (17), (14) is represented as

$$\begin{aligned} \min_{i \in \mathcal{L}_\ell, \ell \geq k} R_{k,i,\ell} &\approx -\frac{1}{\alpha} \log \left(\sum_{\ell=k}^K \sum_{i \in \mathcal{L}_\ell} e^{-\alpha R_{k,i,\ell}} \right) = -\frac{1}{\alpha} \log \left(\sum_{\ell=k}^K \sum_{i \in \mathcal{L}_\ell} e^{-\alpha \log_2 \left(\frac{\bar{\mathbf{f}}^\mathbf{H} \mathbf{A}_{k,i,\ell} \bar{\mathbf{f}}}{\bar{\mathbf{f}}^\mathbf{H} \mathbf{B}_{k,i,\ell} \bar{\mathbf{f}}} \right)} \right) \\ &= -\frac{1}{\alpha} \log \left(\sum_{\ell=k}^K \sum_{i \in \mathcal{L}_\ell} \left(\frac{\bar{\mathbf{f}}^\mathbf{H} \mathbf{A}_{k,i,\ell} \bar{\mathbf{f}}}{\bar{\mathbf{f}}^\mathbf{H} \mathbf{B}_{k,i,\ell} \bar{\mathbf{f}}} \right)^{-\beta} \right), \end{aligned} \quad (20)$$

where $\beta = \alpha \frac{1}{\log 2}$. Similar to this, (15) is obtained as

$$\begin{aligned} \max_{i' \in \mathcal{L}_{\ell'}, \ell' < k} R_{k,i',\ell'} &\approx \frac{1}{\alpha} \log \left(\sum_{\ell'=1}^{k-1} \sum_{i' \in \mathcal{L}_{\ell'}} e^{\alpha R_{k,i',\ell'}} \right) = \frac{1}{\alpha} \log \left(\sum_{\ell'=1}^{k-1} \sum_{i' \in \mathcal{L}_{\ell'}} e^{\alpha \log_2 \left(\frac{\bar{\mathbf{f}}^\mathbf{H} \mathbf{A}_{k,i',\ell'} \bar{\mathbf{f}}}{\bar{\mathbf{f}}^\mathbf{H} \mathbf{B}_{k,i',\ell'} \bar{\mathbf{f}}} \right)} \right) \\ &= \frac{1}{\alpha} \log \left(\sum_{\ell'=1}^{k-1} \sum_{i' \in \mathcal{L}_{\ell'}} \left(\frac{\bar{\mathbf{f}}^\mathbf{H} \mathbf{A}_{k,i',\ell'} \bar{\mathbf{f}}}{\bar{\mathbf{f}}^\mathbf{H} \mathbf{B}_{k,i',\ell'} \bar{\mathbf{f}}} \right)^\beta \right). \end{aligned} \quad (21)$$

Combining (20) and (21), the secrecy rate of the message s_k is approximately

$$\bar{R}_k^{\text{nc}} \approx -\frac{1}{\alpha} \log \left(\sum_{\ell=k}^K \sum_{i \in \mathcal{L}_\ell} \left(\frac{\bar{\mathbf{f}}^\mathbf{H} \mathbf{A}_{k,i,\ell} \bar{\mathbf{f}}}{\bar{\mathbf{f}}^\mathbf{H} \mathbf{B}_{k,i,\ell} \bar{\mathbf{f}}} \right)^{-\beta} \right) - \frac{1}{\alpha} \log \left(\sum_{\ell'=1}^{k-1} \sum_{i' \in \mathcal{L}_{\ell'}} \left(\frac{\bar{\mathbf{f}}^\mathbf{H} \mathbf{A}_{k,i',\ell'} \bar{\mathbf{f}}}{\bar{\mathbf{f}}^\mathbf{H} \mathbf{B}_{k,i',\ell'} \bar{\mathbf{f}}} \right)^\beta \right). \quad (22)$$

Finally, the problem (6) is reformulated as

$$\max_{\bar{\mathbf{f}}} \sum_{k=1}^K \left(-\frac{1}{\alpha} \log \left(\sum_{\ell=k}^K \sum_{i \in \mathcal{L}_\ell} \left(\frac{\bar{\mathbf{f}}^H \mathbf{A}_{k,i,\ell} \bar{\mathbf{f}}}{\bar{\mathbf{f}}^H \mathbf{B}_{k,i,\ell} \bar{\mathbf{f}}} \right)^{-\beta} \right) - \frac{1}{\alpha} \log \left(\sum_{\ell'=1}^{k-1} \sum_{i' \in \mathcal{L}_{\ell'}} \left(\frac{\bar{\mathbf{f}}^H \mathbf{A}_{k,i',\ell'} \bar{\mathbf{f}}}{\bar{\mathbf{f}}^H \mathbf{B}_{k,i',\ell'} \bar{\mathbf{f}}} \right)^\beta \right) \right). \quad (23)$$

We note that the reformulated problem (23) does not contain the transmit power constraint. This is because the objective function in (23) is presented as a form of Rayleigh quotients. Therefore the power constraint $\|\bar{\mathbf{f}}\|$ can be normalized in both of nominator and the denominator without affecting the approximated objective function. Now we are ready to tackle the problem in (23).

B. First-Order KKT Condition

In order to get an insight on the solution of the approximate problem (23), we drive a first-order KKT condition. The following lemma shows the main result in this subsection.

Lemma 1. *In the non-colluding case, the first-order KKT condition of the optimization problem (23) is satisfied if the following holds.*

$$\mathbf{B}_{\text{nc}}^{-1}(\bar{\mathbf{f}}) \mathbf{A}_{\text{nc}}(\bar{\mathbf{f}}) \bar{\mathbf{f}} = \lambda_{\text{nc}}(\bar{\mathbf{f}}) \bar{\mathbf{f}}, \quad (24)$$

where

$$\mathbf{A}_{\text{nc}}(\bar{\mathbf{f}}) = \lambda_{\text{nc}}^{(\text{num})}(\bar{\mathbf{f}}) \times \sum_{k=1}^K \left(\frac{\sum_{\ell=k}^K \sum_{i \in \mathcal{L}_\ell} \left(\beta \left(\frac{\bar{\mathbf{f}}^H \mathbf{A}_{k,i,\ell} \bar{\mathbf{f}}}{\bar{\mathbf{f}}^H \mathbf{B}_{k,i,\ell} \bar{\mathbf{f}}} \right)^{-\beta} \frac{\mathbf{A}_{k,i,\ell}}{\bar{\mathbf{f}}^H \mathbf{A}_{k,i,\ell} \bar{\mathbf{f}}} \right)}{\sum_{\ell=k}^K \sum_{i \in \mathcal{L}_\ell} \left(\frac{\bar{\mathbf{f}}^H \mathbf{A}_{k,i,\ell} \bar{\mathbf{f}}}{\bar{\mathbf{f}}^H \mathbf{B}_{k,i,\ell} \bar{\mathbf{f}}} \right)^{-\beta}} + \frac{\sum_{\ell=1}^{k-1} \sum_{i \in \mathcal{L}_\ell} \left(\beta \left(\frac{\bar{\mathbf{f}}^H \mathbf{A}_{k,i,\ell} \bar{\mathbf{f}}}{\bar{\mathbf{f}}^H \mathbf{B}_{k,i,\ell} \bar{\mathbf{f}}} \right)^\beta \frac{\mathbf{B}_{k,i,\ell}}{\bar{\mathbf{f}}^H \mathbf{B}_{k,i,\ell} \bar{\mathbf{f}}} \right)}{\sum_{\ell=1}^{k-1} \sum_{i \in \mathcal{L}_\ell} \left(\frac{\bar{\mathbf{f}}^H \mathbf{A}_{k,i,\ell} \bar{\mathbf{f}}}{\bar{\mathbf{f}}^H \mathbf{B}_{k,i,\ell} \bar{\mathbf{f}}} \right)^\beta} \right), \quad (25)$$

$$\mathbf{B}_{\text{nc}}(\bar{\mathbf{f}}) = \lambda_{\text{nc}}^{(\text{den})}(\bar{\mathbf{f}}) \times \sum_{k=1}^K \left(\frac{\sum_{\ell=k}^K \sum_{i \in \mathcal{L}_\ell} \left(\beta \left(\frac{\bar{\mathbf{f}}^H \mathbf{A}_{k,i,\ell} \bar{\mathbf{f}}}{\bar{\mathbf{f}}^H \mathbf{B}_{k,i,\ell} \bar{\mathbf{f}}} \right)^{-\beta} \frac{\mathbf{B}_{k,i,\ell}}{\bar{\mathbf{f}}^H \mathbf{B}_{k,i,\ell} \bar{\mathbf{f}}} \right)}{\sum_{\ell=k}^K \sum_{i \in \mathcal{L}_\ell} \left(\frac{\bar{\mathbf{f}}^H \mathbf{A}_{k,i,\ell} \bar{\mathbf{f}}}{\bar{\mathbf{f}}^H \mathbf{B}_{k,i,\ell} \bar{\mathbf{f}}} \right)^{-\beta}} + \frac{\sum_{\ell=1}^{k-1} \sum_{i \in \mathcal{L}_\ell} \left(\beta \left(\frac{\bar{\mathbf{f}}^H \mathbf{A}_{k,i,\ell} \bar{\mathbf{f}}}{\bar{\mathbf{f}}^H \mathbf{B}_{k,i,\ell} \bar{\mathbf{f}}} \right)^\beta \frac{\mathbf{A}_{k,i,\ell}}{\bar{\mathbf{f}}^H \mathbf{A}_{k,i,\ell} \bar{\mathbf{f}}} \right)}{\sum_{\ell=1}^{k-1} \sum_{i \in \mathcal{L}_\ell} \left(\frac{\bar{\mathbf{f}}^H \mathbf{A}_{k,i,\ell} \bar{\mathbf{f}}}{\bar{\mathbf{f}}^H \mathbf{B}_{k,i,\ell} \bar{\mathbf{f}}} \right)^\beta} \right), \quad (26)$$

with

$$\lambda_{\text{nc}}(\bar{\mathbf{f}}) = \sum_{k=1}^K \left(-\frac{1}{\alpha} \log \left(\sum_{\ell=k}^K \sum_{i \in \mathcal{L}_\ell} \left(\frac{\bar{\mathbf{f}}^H \mathbf{A}_{k,i,\ell} \bar{\mathbf{f}}}{\bar{\mathbf{f}}^H \mathbf{B}_{k,i,\ell} \bar{\mathbf{f}}} \right)^{-\beta} \right) - \frac{1}{\alpha} \log \left(\sum_{\ell'=1}^{k-1} \sum_{i' \in \mathcal{L}_{\ell'}} \left(\frac{\bar{\mathbf{f}}^H \mathbf{A}_{k,i',\ell'} \bar{\mathbf{f}}}{\bar{\mathbf{f}}^H \mathbf{B}_{k,i',\ell'} \bar{\mathbf{f}}} \right)^\beta \right) \right) \quad (27)$$

$$= \frac{\lambda_{\text{nc}}^{(\text{num})}(\bar{\mathbf{f}})}{\lambda_{\text{nc}}^{(\text{den})}(\bar{\mathbf{f}})}. \quad (28)$$

Proof. See Appendix A.1. □

Now we interpret the derived optimality condition (24). If the precoding vector $\bar{\mathbf{f}}$ satisfies (24), it satisfies the first-order optimality condition, implying that $\bar{\mathbf{f}}$ is located on a stationary point that has zero-gradient. This, however, does not guarantee that $\bar{\mathbf{f}}$ is a good solution. Among such points, we need to find a local optimal point that maximizes the objective function of (23). To this end, we first observe that (24) can be cast as a generalized eigenvalue problem. Rigorously, (24) is interpreted as a class of a eigenvector dependent nonlinear eigenvalue problem (NEPv) [26]. A distinguishable feature of NEPv compared to a typical eigenvalue problem is that a matrix is a function of eigenvectors. Based on this interpretation, $\mathbf{B}_{\text{nc}}^{-1}(\bar{\mathbf{f}})\mathbf{A}_{\text{nc}}(\bar{\mathbf{f}})$ behaves as the corresponding matrix, $\bar{\mathbf{f}}$ behaves as the eigenvector of the matrix $\mathbf{B}_{\text{nc}}^{-1}(\bar{\mathbf{f}})\mathbf{A}_{\text{nc}}(\bar{\mathbf{f}})$, and $\lambda_{\text{nc}}(\bar{\mathbf{f}})$ behaves as the eigenvalue. Noticeably, the eigenvalue $\lambda_{\text{nc}}(\bar{\mathbf{f}})$ is equivalent with the objective function that we want to maximize. For this reason, if we find the principal eigenvector of $\mathbf{B}_{\text{nc}}^{-1}(\bar{\mathbf{f}})\mathbf{A}_{\text{nc}}(\bar{\mathbf{f}})$, then it maximizes our objective function of (23) while satisfying (24). Consequently, finding the principal eigenvector of $\mathbf{B}_{\text{nc}}^{-1}(\bar{\mathbf{f}})\mathbf{A}_{\text{nc}}(\bar{\mathbf{f}})$ is equivalent to finding the best local optimal point.

Finding the principal eigenvector of $\mathbf{B}_{\text{nc}}^{-1}(\bar{\mathbf{f}})\mathbf{A}_{\text{nc}}(\bar{\mathbf{f}})$ is far from trivial. A main challenge comes from that the matrix $\mathbf{B}_{\text{nc}}^{-1}(\bar{\mathbf{f}})\mathbf{A}_{\text{nc}}(\bar{\mathbf{f}})$ changes depending on $\bar{\mathbf{f}}$. In the next subsection, we propose a novel method called GPI-HIA for the non-colluding case (GPI-HIA (Non-Coll)) so as to efficiently obtain the principal eigenvector.

C. GPI-HIA for the Non-Colluding Case

We present the GPI-HIA (Non-Coll) method. Inspired from the typical power iteration method, the proposed method iteratively updates the precoding vector $\bar{\mathbf{f}}$ as

$$\bar{\mathbf{f}}_{(t)} \leftarrow \frac{\mathbf{B}_{\text{nc}}^{-1}(\bar{\mathbf{f}}_{(t-1)})\mathbf{A}_{\text{nc}}(\bar{\mathbf{f}}_{(t-1)})\bar{\mathbf{f}}_{(t-1)}}{\|\mathbf{B}_{\text{nc}}^{-1}(\bar{\mathbf{f}}_{(t-1)})\mathbf{A}_{\text{nc}}(\bar{\mathbf{f}}_{(t-1)})\bar{\mathbf{f}}_{(t-1)}\|}. \quad (29)$$

We repeat this process until the convergence criterion is met. The convergence condition is $\|\bar{\mathbf{f}}_{(t)} - \bar{\mathbf{f}}_{(t-1)}\| < \epsilon$, where ϵ is the tolerance level. Algorithm 1 summarizes the process.

Remark 2. (α tuning) The parameter α determines the accuracy of the LogSumExp approximation. As we use large α , the approximation becomes tight; thereby using large α is desirable. Nevertheless, as presented in [27], too large α may make the proposed GPI-HIA algorithm not converge. This is because, as α increases, the LogSumExp function becomes more similar to the minimum function and its shape turns to be non-smooth. In this case, no stationary point is characterized; thus, the algorithm cannot find the converging point.

Algorithm 1: GPI-HIA (Non-Coll)

```

1 initialize:  $\bar{\mathbf{f}}_{(0)}$  (MRT)
2 Set the iteration count  $t = 1$ 
3 while  $\|\bar{\mathbf{f}}_{(t)} - \bar{\mathbf{f}}_{(t-1)}\| > \epsilon$  do
4   Construct the matrix  $\mathbf{A}_{\text{nc}}(\bar{\mathbf{f}}_{(t-1)})$  by using (25).
5   Construct the matrix  $\mathbf{B}_{\text{nc}}(\bar{\mathbf{f}}_{(t-1)})$  by using (26).
6   Compute  $\bar{\mathbf{f}}_{(t)} = \mathbf{B}_{\text{nc}}^{-1}(\bar{\mathbf{f}}_{(t-1)})\mathbf{A}_{\text{nc}}(\bar{\mathbf{f}}_{(t-1)})\bar{\mathbf{f}}_{(t-1)}$ .
7   Normalize  $\bar{\mathbf{f}}_{(t)} = \bar{\mathbf{f}}_{(t)} / \|\bar{\mathbf{f}}_{(t)}\|$ .
8    $t \leftarrow t + 1$ .
9 return  $\bar{\mathbf{f}} = \bar{\mathbf{f}}_{(t)}$ .

```

To properly tune α , we use the following method. We start the GPI-HIA with large α . If the iteration loop of the GPI-HIA does not converge within the predetermined number of iterations, we regard that the used α is too large to make the algorithm converge, so that we enforce to terminate the loop, decrease α with the predetermined amount, and newly start the algorithm again. We repeat this process until the algorithm converges before the predetermined number. As shown in the later section, the GPI-HIA algorithm with this α tuning performs very well.

Remark 3 (Complexity and implementation). Similar to [27]–[29], the computational complexity is dominated by calculating $\mathbf{B}_{\text{nc}}^{-1}(\bar{\mathbf{f}})$. Since $\mathbf{B}_{\text{nc}}(\bar{\mathbf{f}})$ is a block-diagonal matrix that consists of K number of $N \times N$ sub-matrices, its inverse can be obtained by acquiring the inversion of each sub-matrix. Accordingly, the computational complexity per iteration is analyzed as $O(KN^3)$.

We emphasize on that the proposed method has a benefit in implementation. For example, in [5] where a transmit power minimization for the HIA model was tackled, a non-convex original problem was relaxed into a convex form and CVX was exploited to get a solution. Nevertheless, since CVX is not designed to run in real-time FPGA hardware [30], it is infeasible to use this convex relaxation-based method in practice. On the contrary, our method does not need to use any off-the-shelf solver including CVX. The only required computational load is the matrix inversion, which is also used in a very simple precoding strategy such as ZF. For this reason, our method is preferable in terms of implementation compared to conventional convex relaxation based approaches.

D. Fairness

One possible issue in the HIA model is fairness. Since we maximize the sum secrecy rate, users in a certain layer may suffer from a very low rate. For example, increasing the power of the high priority messages incurs critical interference to the lower priority users, while increasing the power of the low priority messages is not harmful because the high priority users can eliminate the low priority messages via SIC. For this reason, in a perspective of the sum secrecy rate maximization, it is beneficial to increase the power of the low priority messages and decrease the secrecy rate of the high priority users, which can lead to an undesirable rate distribution in terms of fairness.

To resolve this fairness issue, we modify the proposed GPI-HIA (Non-Coll) by adopting the proportional fairness (PF) policy [31]. In the PF algorithm, the BS traces the previously served rate on average and reflects this value into the optimization problem as inverse weights. Specifically, denoting that $\bar{R}_k^{\text{nc}}(t)$ as the achieved secrecy rate for the message s_k in the transmission block t , the average secrecy rate $\mu_k^{\text{nc}}(t+1)$ is updated by a simple first-order autoregressive filter as

$$\mu_k^{\text{nc}}(t+1) = (1 - \delta)\mu_k^{\text{nc}}(t) + \delta\bar{R}_k^{\text{nc}}(t), \quad (30)$$

where $\delta \in (0, 1)$ is a given parameter. With $\mu_k^{\text{nc}}(t)$, we modify the problem (6) into the weighted sum secrecy rate maximization problem as

$$\max_{\mathbf{f}_1, \dots, \mathbf{f}_K} \sum_{k=1}^K \frac{1}{\mu_k^{\text{nc}}(t)} \bar{R}_k^{\text{nc}} \quad (31)$$

$$\text{subject to } \sum_{k=1}^K \|\mathbf{f}_k\|^2 = 1. \quad (32)$$

By doing this, if the message s_k has obtained very small secrecy rate during the previous transmission periods, $\mu_k^{\text{nc}}(t)$ decreases. This leads to the increase in the weight of \bar{R}_k^{nc} . Then the BS tends to increase \bar{R}_k^{nc} considerably in the next transmission period. On the contrary to that, if the message s_k has obtained large secrecy rate during the previous transmission periods, the PF algorithm puts a little efforts into increasing \bar{R}_k^{nc} , so as to provide the secrecy rate fairly.

To obtain a solution of the modified weighted sum secrecy rate maximization problem (31), the corresponding first-order optimality condition is derived as follows.

Corollary 1. *In the non-colluding case, the first-order KKT condition of the modified optimization problem (31) is satisfied if the following holds.*

$$\bar{\mathbf{B}}_{\text{nc}}^{-1}(\bar{\mathbf{f}})\bar{\mathbf{A}}_{\text{nc}}(\bar{\mathbf{f}})\bar{\mathbf{f}} = \bar{\lambda}_{\text{nc}}(\bar{\mathbf{f}})\bar{\mathbf{f}}, \quad (33)$$

where

$$\bar{\mathbf{A}}_{\text{nc}}(\bar{\mathbf{f}}) = \bar{\lambda}_{\text{nc}}^{(\text{num})}(\bar{\mathbf{f}}) \times \sum_{k=1}^K \frac{1}{\mu_k^{\text{nc}}(t)} \left(\frac{\sum_{\ell=k}^K \sum_{i \in \mathcal{L}_\ell} \left(\beta \left(\frac{\bar{\mathbf{f}}^H \mathbf{A}_{k,i,\ell} \bar{\mathbf{f}}}{\bar{\mathbf{f}}^H \mathbf{B}_{k,i,\ell} \bar{\mathbf{f}}} \right)^{-\beta} \frac{\mathbf{A}_{k,i,\ell}}{\bar{\mathbf{f}}^H \mathbf{A}_{k,i,\ell} \bar{\mathbf{f}}} \right)}{\sum_{\ell=k}^K \sum_{i \in \mathcal{L}_\ell} \left(\frac{\bar{\mathbf{f}}^H \mathbf{A}_{k,i,\ell} \bar{\mathbf{f}}}{\bar{\mathbf{f}}^H \mathbf{B}_{k,i,\ell} \bar{\mathbf{f}}} \right)^{-\beta}} + \frac{\sum_{\ell=1}^{k-1} \sum_{i \in \mathcal{L}_\ell} \left(\beta \left(\frac{\bar{\mathbf{f}}^H \mathbf{A}_{k,i,\ell} \bar{\mathbf{f}}}{\bar{\mathbf{f}}^H \mathbf{B}_{k,i,\ell} \bar{\mathbf{f}}} \right)^\beta \frac{\mathbf{B}_{k,i,\ell}}{\bar{\mathbf{f}}^H \mathbf{B}_{k,i,\ell} \bar{\mathbf{f}}} \right)}{\sum_{\ell=1}^{k-1} \sum_{i \in \mathcal{L}_\ell} \left(\frac{\bar{\mathbf{f}}^H \mathbf{A}_{k,i,\ell} \bar{\mathbf{f}}}{\bar{\mathbf{f}}^H \mathbf{B}_{k,i,\ell} \bar{\mathbf{f}}} \right)^\beta} \right), \quad (34)$$

$$\bar{\mathbf{B}}_{\text{nc}}(\bar{\mathbf{f}}) = \bar{\lambda}_{\text{nc}}^{(\text{den})}(\bar{\mathbf{f}}) \times \sum_{k=1}^K \frac{1}{\mu_k^{\text{nc}}(t)} \left(\frac{\sum_{\ell=k}^K \sum_{i \in \mathcal{L}_\ell} \left(\beta \left(\frac{\bar{\mathbf{f}}^H \mathbf{A}_{k,i,\ell} \bar{\mathbf{f}}}{\bar{\mathbf{f}}^H \mathbf{B}_{k,i,\ell} \bar{\mathbf{f}}} \right)^{-\beta} \frac{\mathbf{B}_{k,i,\ell}}{\bar{\mathbf{f}}^H \mathbf{B}_{k,i,\ell} \bar{\mathbf{f}}} \right)}{\sum_{\ell=k}^K \sum_{i \in \mathcal{L}_\ell} \left(\frac{\bar{\mathbf{f}}^H \mathbf{A}_{k,i,\ell} \bar{\mathbf{f}}}{\bar{\mathbf{f}}^H \mathbf{B}_{k,i,\ell} \bar{\mathbf{f}}} \right)^{-\beta}} + \frac{\sum_{\ell=1}^{k-1} \sum_{i \in \mathcal{L}_\ell} \left(\beta \left(\frac{\bar{\mathbf{f}}^H \mathbf{A}_{k,i,\ell} \bar{\mathbf{f}}}{\bar{\mathbf{f}}^H \mathbf{B}_{k,i,\ell} \bar{\mathbf{f}}} \right)^\beta \frac{\mathbf{A}_{k,i,\ell}}{\bar{\mathbf{f}}^H \mathbf{A}_{k,i,\ell} \bar{\mathbf{f}}} \right)}{\sum_{\ell=1}^{k-1} \sum_{i \in \mathcal{L}_\ell} \left(\frac{\bar{\mathbf{f}}^H \mathbf{A}_{k,i,\ell} \bar{\mathbf{f}}}{\bar{\mathbf{f}}^H \mathbf{B}_{k,i,\ell} \bar{\mathbf{f}}} \right)^\beta} \right), \quad (35)$$

and

$$\bar{\lambda}_{\text{nc}}(\bar{\mathbf{f}}) = \sum_{k=1}^K \frac{1}{\mu_k^{\text{nc}}(t)} \left(-\frac{1}{\alpha} \log \left(\sum_{\ell=k}^K \sum_{i \in \mathcal{L}_\ell} \left(\frac{\bar{\mathbf{f}}^H \mathbf{A}_{k,i,\ell} \bar{\mathbf{f}}}{\bar{\mathbf{f}}^H \mathbf{B}_{k,i,\ell} \bar{\mathbf{f}}} \right)^{-\beta} \right) - \frac{1}{\alpha} \log \left(\sum_{\ell'=1}^{k-1} \sum_{i' \in \mathcal{L}_{\ell'}} \left(\frac{\bar{\mathbf{f}}^H \mathbf{A}_{k,i',\ell'} \bar{\mathbf{f}}}{\bar{\mathbf{f}}^H \mathbf{B}_{k,i',\ell'} \bar{\mathbf{f}}} \right)^\beta \right) \right) \quad (36)$$

$$= \frac{\bar{\lambda}_{\text{nc}}^{(\text{num})}(\bar{\mathbf{f}})}{\bar{\lambda}_{\text{nc}}^{(\text{den})}(\bar{\mathbf{f}})}. \quad (37)$$

Proof. The proof is straightforward by adding the weight $1/\mu_k^{\text{nc}}(t)$ to the partial derivative of $\lambda_{\text{nc}}(\bar{\mathbf{f}})$ in Appendix A.1. \square

Using Corollary 1, the proposed GPI-HIA (Non-Coll) with the PF policy follows similar steps to Algorithm 1: Step 1. we compute the precoding vector using GPI-HIA, i.e., the principal eigenvector of $\bar{\mathbf{B}}_{\text{nc}}^{-1}(\bar{\mathbf{f}})\bar{\mathbf{A}}_{\text{nc}}(\bar{\mathbf{f}})$, Step 2. update $\mu_k^{\text{nc}}(t)$ according to (30), and Step 3. repeat the steps 1 to 2. In the later section, we show that the proposed GPI-HIA adopting the PF policy achieves much improved fairness.

IV. PRECODING OPTIMIZATION IN THE COLLUDING CASE

In this section, we consider the colluding case assuming that the lower priority users cooperate to decode the high priority message. To solve the optimization problem in (10) which is formulated for the colluding case, similar to the non-colluding case, we first convert the minimum function involved in (10) using the LogSumExp technique. Subsequently, we reformulate the approximated problem as a form of Rayleigh quotients with regard to the high dimensional

vector (16). With this form, we drive the first-order optimality condition and propose a novel algorithm to obtain the principal eigenvector.

A. Reformulation to a Tractable Form

A difference of the colluding case compared to the non-colluding case is on the achievable rate of the wiretapping channel. The achievable rate of the colluding wiretapping channel is

$$\begin{aligned}
R_{k,i',\ell'}^e &= \log_2 \left(1 + \sum_{\ell'=1}^{k-1} \sum_{i' \in \mathcal{L}_{\ell'}} \frac{|\mathbf{h}_{i',\ell'}^H \mathbf{f}_k|^2}{\sum_{j=k+1}^K |\mathbf{h}_{i',\ell'}^H \mathbf{f}_j|^2 + \frac{\sigma^2}{P}} \right) \\
&= \log_2 \left(\sum_{\ell'=1}^{k-1} \sum_{i' \in \mathcal{L}_{\ell'}} \left(\frac{\sum_{j=k}^K \mathbf{f}_j^H \mathbf{h}_{i',\ell'} \mathbf{h}_{i',\ell'}^H \mathbf{f}_j + \frac{\sigma^2}{P}}{\sum_{j=k+1}^K \mathbf{f}_j^H \mathbf{h}_{i',\ell'} \mathbf{h}_{i',\ell'}^H \mathbf{f}_j + \frac{\sigma^2}{P}} + \frac{1}{\gamma_k} \right) \right) = \frac{1}{\log 2} \log \left(\sum_{\ell'=1}^{k-1} \sum_{i' \in \mathcal{L}_{\ell'}} \left(\frac{\bar{\mathbf{f}}^H \mathbf{C}_{k,i',\ell'} \bar{\mathbf{f}}}{\bar{\mathbf{f}}^H \mathbf{D}_{k,i',\ell'} \bar{\mathbf{f}}} \right) \right),
\end{aligned} \tag{38}$$

where

$$\mathbf{C}_{k,i',\ell'} = \text{blkdiag} \left(\mathbf{0}, \dots, \mathbf{0}, \underbrace{\gamma_k \mathbf{h}_{i',\ell'} \mathbf{h}_{i',\ell'}^H}_{k\text{th block}}, \mathbf{h}_{i',\ell'} \mathbf{h}_{i',\ell'}^H, \dots, \mathbf{h}_{i',\ell'} \mathbf{h}_{i',\ell'}^H \right) + \frac{\sigma^2}{P} \mathbf{I}_{NK}, \tag{39}$$

$$\mathbf{D}_{k,i',\ell'} = \gamma_k \times \text{blkdiag} \left(\mathbf{0}, \dots, \mathbf{0}, \underbrace{\mathbf{h}_{i',\ell'} \mathbf{h}_{i',\ell'}^H}_{(k+1)\text{th block}}, \dots, \mathbf{h}_{i',\ell'} \mathbf{h}_{i',\ell'}^H \right) + \frac{\gamma_k \sigma^2}{P} \mathbf{I}_{NK}. \tag{40}$$

and $\gamma_k = \sum_{\ell'=1}^{k-1} |\mathcal{L}_{\ell'}|$. Combining (20) and (38), the secrecy rate of the message s_k is approximately

$$\bar{R}_k^c \approx -\frac{1}{\alpha} \log \left(\sum_{\ell=k}^K \sum_{i \in \mathcal{L}_{\ell}} \left(\frac{\bar{\mathbf{f}}^H \mathbf{A}_{k,i,\ell} \bar{\mathbf{f}}}{\bar{\mathbf{f}}^H \mathbf{B}_{k,i,\ell} \bar{\mathbf{f}}} \right)^{-\beta} \right) - \frac{1}{\log 2} \log \left(\sum_{\ell'=1}^{k-1} \sum_{i' \in \mathcal{L}_{\ell'}} \left(\frac{\bar{\mathbf{f}}^H \mathbf{C}_{k,i',\ell'} \bar{\mathbf{f}}}{\bar{\mathbf{f}}^H \mathbf{D}_{k,i',\ell'} \bar{\mathbf{f}}} \right) \right). \tag{41}$$

Finally, with these high dimensional representations, the problem (10) is reformulated as

$$\max_{\bar{\mathbf{f}}} \sum_{k=1}^K \left(-\frac{1}{\alpha} \log \left(\sum_{\ell=k}^K \sum_{i \in \mathcal{L}_{\ell}} \left(\frac{\bar{\mathbf{f}}^H \mathbf{A}_{k,i,\ell} \bar{\mathbf{f}}}{\bar{\mathbf{f}}^H \mathbf{B}_{k,i,\ell} \bar{\mathbf{f}}} \right)^{-\beta} \right) - \frac{1}{\log 2} \log \left(\sum_{\ell'=1}^{k-1} \sum_{i' \in \mathcal{L}_{\ell'}} \left(\frac{\bar{\mathbf{f}}^H \mathbf{C}_{k,i',\ell'} \bar{\mathbf{f}}}{\bar{\mathbf{f}}^H \mathbf{D}_{k,i',\ell'} \bar{\mathbf{f}}} \right) \right) \right). \tag{42}$$

The transmit power constraint vanishes in (42) because when reformulating the objective equation into form of Rayleigh quotients as (42), numerator and denominator are normalized by $\|\bar{\mathbf{f}}\|$ without affecting the objective equation. Now we are ready to tackle the problem (42).

B. First-Order KKT Condition

In order to obtain a solution of (42), we derive a first-order KKT condition. The following lemma shows the main result in this subsection.

Lemma 2. *In the colluding case, the first-order KKT condition of the optimization problem (42) is satisfied if the following holds.*

$$\mathbf{B}_c^{-1}(\bar{\mathbf{f}})\mathbf{A}_c(\bar{\mathbf{f}}) = \lambda_c(\bar{\mathbf{f}})\bar{\mathbf{f}} \quad (43)$$

where

$$\mathbf{A}_c(\bar{\mathbf{f}}) = \lambda_c^{(\text{num})} \times \sum_{k=1}^K \left(\frac{1}{\alpha} \frac{\sum_{\ell=k}^K \sum_{i \in \mathcal{L}_\ell} \beta \left(\frac{\bar{\mathbf{f}}^H \mathbf{A}_{k,i,\ell} \bar{\mathbf{f}}}{\bar{\mathbf{f}}^H \mathbf{B}_{k,i,\ell} \bar{\mathbf{f}}} \right)^{-\beta} \mathbf{A}_{k,i,\ell}}{\sum_{\ell=k}^K \sum_{i \in \mathcal{L}_\ell} \left(\frac{\bar{\mathbf{f}}^H \mathbf{A}_{k,i,\ell} \bar{\mathbf{f}}}{\bar{\mathbf{f}}^H \mathbf{B}_{k,i,\ell} \bar{\mathbf{f}}} \right)^{-\beta}} + \frac{1}{\log 2} \frac{\sum_{\ell'=1}^{k-1} \sum_{i' \in \mathcal{L}_{\ell'}} \frac{\bar{\mathbf{f}}^H \mathbf{C}_{k,i',\ell'} \bar{\mathbf{f}}}{\bar{\mathbf{f}}^H \mathbf{D}_{k,i',\ell'} \bar{\mathbf{f}}} \left(\frac{\mathbf{D}_{k,i',\ell'}}{\bar{\mathbf{f}}^H \mathbf{D}_{k,i',\ell'} \bar{\mathbf{f}}} \right)}{\sum_{\ell'=1}^{k-1} \sum_{i' \in \mathcal{L}_{\ell'}} \frac{\bar{\mathbf{f}}^H \mathbf{C}_{k,i',\ell'} \bar{\mathbf{f}}}{\bar{\mathbf{f}}^H \mathbf{D}_{k,i',\ell'} \bar{\mathbf{f}}}} \right), \quad (44)$$

$$\mathbf{B}_c(\bar{\mathbf{f}}) = \lambda_c^{(\text{den})} \times \sum_{k=1}^K \left(\frac{1}{\alpha} \frac{\sum_{\ell=k}^K \sum_{i \in \mathcal{L}_\ell} \beta \left(\frac{\bar{\mathbf{f}}^H \mathbf{A}_{k,i,\ell} \bar{\mathbf{f}}}{\bar{\mathbf{f}}^H \mathbf{B}_{k,i,\ell} \bar{\mathbf{f}}} \right)^{-\beta} \mathbf{B}_{k,i,\ell}}{\sum_{\ell=k}^K \sum_{i \in \mathcal{L}_\ell} \left(\frac{\bar{\mathbf{f}}^H \mathbf{A}_{k,i,\ell} \bar{\mathbf{f}}}{\bar{\mathbf{f}}^H \mathbf{B}_{k,i,\ell} \bar{\mathbf{f}}} \right)^{-\beta}} + \frac{1}{\log 2} \frac{\sum_{\ell'=1}^{k-1} \sum_{i' \in \mathcal{L}_{\ell'}} \frac{\bar{\mathbf{f}}^H \mathbf{C}_{k,i',\ell'} \bar{\mathbf{f}}}{\bar{\mathbf{f}}^H \mathbf{D}_{k,i',\ell'} \bar{\mathbf{f}}} \left(\frac{\mathbf{C}_{k,i',\ell'}}{\bar{\mathbf{f}}^H \mathbf{C}_{k,i',\ell'} \bar{\mathbf{f}}} \right)}{\sum_{\ell'=1}^{k-1} \sum_{i' \in \mathcal{L}_{\ell'}} \frac{\bar{\mathbf{f}}^H \mathbf{C}_{k,i',\ell'} \bar{\mathbf{f}}}{\bar{\mathbf{f}}^H \mathbf{D}_{k,i',\ell'} \bar{\mathbf{f}}}} \right), \quad (45)$$

with

$$\lambda_c(\bar{\mathbf{f}}) = \sum_{k=1}^K \left(-\frac{1}{\alpha} \log \left(\sum_{\ell=k}^K \sum_{i \in \mathcal{L}_\ell} \left(\frac{\bar{\mathbf{f}}^H \mathbf{A}_{k,i,\ell} \bar{\mathbf{f}}}{\bar{\mathbf{f}}^H \mathbf{B}_{k,i,\ell} \bar{\mathbf{f}}} \right)^{-\beta} \right) - \frac{1}{\log 2} \log \left(\sum_{\ell'=1}^{k-1} \sum_{i' \in \mathcal{L}_{\ell'}} \left(\frac{\bar{\mathbf{f}}^H \mathbf{C}_{k,i',\ell'} \bar{\mathbf{f}}}{\bar{\mathbf{f}}^H \mathbf{D}_{k,i',\ell'} \bar{\mathbf{f}}} \right) \right) \right) \quad (46)$$

$$= \frac{\lambda_c^{(\text{num})}(\bar{\mathbf{f}})}{\lambda_c^{(\text{den})}(\bar{\mathbf{f}})}. \quad (47)$$

Proof. See Appendix A.2. □

Similar to the non-colluding case, the derived optimality condition (42) is cast as a class of NEPv [26] where the corresponding eigenvalue is equivalent to the objective function of (10). Consequently, finding the principal eigenvector of $\mathbf{B}_c^{-1}(\bar{\mathbf{f}})\mathbf{A}_c(\bar{\mathbf{f}})$ is equivalent to finding the local optimal point. In the next subsection, we propose a novel method GPI-HIA for the colluding case (GPI-HIA (Coll)) which finds the principal eigenvector efficiently.

C. GPI-HIA for the Colluding Case

The proposed GPI-HIA (Coll) iteratively updates the precoding vector as

$$\bar{\mathbf{f}}_{(t)} \leftarrow \frac{\mathbf{B}_c^{-1}(\bar{\mathbf{f}}_{(t-1)})\mathbf{A}_c(\bar{\mathbf{f}}_{(t-1)})\bar{\mathbf{f}}_{(t-1)}}{\|\mathbf{B}_c^{-1}(\bar{\mathbf{f}}_{(t-1)})\mathbf{A}_c(\bar{\mathbf{f}}_{(t-1)})\bar{\mathbf{f}}_{(t-1)}\|}. \quad (48)$$

Algorithm 2: GPI-HIA (Coll)

```

1 initialize:  $\bar{\mathbf{f}}_{(0)}$  (MRT)
2 Set the iteration count  $t = 1$ 
3 while  $\|\bar{\mathbf{f}}_{(t)} - \bar{\mathbf{f}}_{(t-1)}\| > \epsilon$  do
4   Construct the matrix  $\mathbf{A}_c(\bar{\mathbf{f}}_{(t-1)})$  by using (44).
5   Construct the matrix  $\mathbf{B}_c(\bar{\mathbf{f}}_{(t-1)})$  by using (45).
6   Compute  $\bar{\mathbf{f}}_{(t)} = \mathbf{B}_c^{-1}(\bar{\mathbf{f}}_{(t-1)})\mathbf{A}_c(\bar{\mathbf{f}}_{(t-1)})\bar{\mathbf{f}}_{(t-1)}$ .
7   Normalize  $\bar{\mathbf{f}}_{(t)} = \bar{\mathbf{f}}_{(t)} / \|\bar{\mathbf{f}}_{(t)}\|$ .
8    $t \leftarrow t + 1$ .
9 return  $\bar{\mathbf{f}} = \bar{\mathbf{f}}_{(t)}$ .

```

We repeat this process until the convergence criterion is met. For the convergence condition, we use $\|\bar{\mathbf{f}}_{(t)} - \bar{\mathbf{f}}_{(t-1)}\| < \epsilon$ where ϵ is a tolerance level. Algorithm 2 describes the process.

Remark 4. (Fairness) The fairness issue can be caused in the colluding case by an imbalance between the lower layer users' rates and the higher layer users' rates. We can address this issue by adopting the PF policy as in the non-colluding HIA case.

V. SPECIAL CASE: PRECODING OPTIMIZATION IN DOWNLINK NOMA SYSTEMS

As a special case, our problems can reduce to a sum rate maximization problem in downlink MISO NOMA systems. In downlink MISO NOMA, each user has interference decoding capability in order to mitigate the amount of inter-user interference. Specifically, assuming that the BS serves K users and the decoding order at each user is predetermined as $1 \rightarrow K$, user k first decodes s_1, \dots, s_{k-1} and removes the decoded messages, and decodes s_k with the reduced amount of the interference. Without loss of generality, we let $|\mathbf{h}_1|^2 < |\mathbf{h}_2|^2 < \dots < |\mathbf{h}_K|^2$. To properly perform this SIC, it needs to be guaranteed that user k successfully decodes s_1, \dots, s_{k-1} , leading to that the information rate of s_k is determined as $\bar{R}_k = \min_{i \geq k} \{R_{i,k}\}$, where $R_{i,k}$ is the achievable rate of user i for the message s_k defined as [23]

$$R_{i,k} = \log_2 \left(1 + \frac{|\mathbf{h}_i^H \mathbf{f}_k|^2}{\sum_{j=k+1}^K |\mathbf{h}_i^H \mathbf{f}_j|^2 + \frac{\sigma^2}{P}} \right). \quad (49)$$

In (49), \mathbf{h}_i is the channel vector between the BS and user i . Maximizing the sum rate in this system, an optimization problem with respect to the precoders is formulated as

$$\max_{\mathbf{f}_1, \dots, \mathbf{f}_K} \sum_{k=1}^K \bar{R}_k \quad (50)$$

$$\text{subject to } \sum_{k=1}^K \|\mathbf{f}_k\|^2 = 1. \quad (51)$$

Comparing (6), (10), and (50), we observe that the problem (50) is equivalent to the simplified form of our original setup, that can be reduced by ignoring the wiretapping lower priority users and assuming that only one user exists in each layer, i.e., $|\mathcal{L}_i| = 1$ for $i \in \{1, \dots, K\}$. For this reason, the proposed GPI-HIA method is also applicable for optimizing downlink MISO NOMA systems. In this section, extending our method further, we investigate how to apply the proposed method to solve (50) under the imperfect CSIT assumption.

A. CSIT Acquisition and Relaxation

On the contrary to the previous sections, we assume that the BS cannot have perfect knowledge of CSIT. Specifically, a limited feedback strategy is used to acquire the corresponding CSIT [32], [33], which renders the estimated CSIT $\hat{\mathbf{h}}_i$ as follows:

$$\hat{\mathbf{h}}_i = \mathbf{U}_i \Lambda_i^{\frac{1}{2}} \left(\sqrt{1 - \kappa^2} \mathbf{g}_i + \kappa \mathbf{v}_i \right) = \mathbf{h}_i - \mathbf{e}_i, \quad (52)$$

where \mathbf{e}_i is the CSIT estimation error, \mathbf{U}_i and Λ_i is the set of eigenvectors and eigenvalues of channel covariance matrix, \mathbf{g}_i and \mathbf{v}_i are drawn from IID $CN(0, 1)$. Here, the amount of feedback bits is implicitly controlled via the parameter κ ; so that κ decreases when the feedback bits increase, thereby the CSIT accuracy increases. In (52), the covariance of the error \mathbf{e}_i is

$$\mathbb{E}[\mathbf{e}_i \mathbf{e}_i^H] = \mathbf{U}_i \Lambda_i^{\frac{1}{2}} \left(2 - 2\sqrt{1 - \kappa^2} \right) \Lambda_i^{\frac{1}{2}} \mathbf{U}_i^H = \Phi_i. \quad (53)$$

With estimated channel vector, a lower bound on the achievable rate is obtained as

$$\begin{aligned} R_{i,k} &= \mathbb{E} \left[\log_2 \left(1 + \frac{|\mathbf{h}_i^H \mathbf{f}_k|^2}{\sum_{j=k+1}^K |\mathbf{h}_i^H \mathbf{f}_j|^2 + \frac{\sigma^2}{P}} \right) \right] \\ &\stackrel{(a)}{\geq} \log_2 \left(1 + \frac{\mathbf{f}_k^H \hat{\mathbf{h}}_i \hat{\mathbf{h}}_i^H \mathbf{f}_k}{\sum_{j=k+1}^K \mathbf{f}_j^H \hat{\mathbf{h}}_i \hat{\mathbf{h}}_i^H \mathbf{f}_j + \sum_{j=k}^K \mathbf{f}_j^H \mathbb{E}[\mathbf{e}_i \mathbf{e}_i^H] \mathbf{f}_j + \frac{\sigma^2}{P}} \right) \\ &= \log_2 \left(1 + \frac{\mathbf{f}_k^H \hat{\mathbf{h}}_i \hat{\mathbf{h}}_i^H \mathbf{f}_k}{\sum_{j=k+1}^K \mathbf{f}_j^H \hat{\mathbf{h}}_i \hat{\mathbf{h}}_i^H \mathbf{f}_j + \sum_{j=k}^K \mathbf{f}_j^H \Phi_i \mathbf{f}_j + \frac{\sigma^2}{P}} \right) = R_{i,k}^{\text{lb}}, \end{aligned} \quad (54)$$

where the expectation is for the randomness associated with the CSIT error, and (a) comes from treating the CSIT estimation error as additive noise [27], [29] and applying Jensen's inequality. With (54), a lower bound on the information rate of s_k is set as $\bar{R}_k^{\text{lb}} = \min_{i \geq k} \{R_{i,k}^{\text{lb}}\}$. Accordingly, a relaxed sum rate maximization problem in NOMA system is reformulated as

$$\max_{\mathbf{f}_1, \dots, \mathbf{f}_K} \sum_{k=1}^K \bar{R}_k^{\text{lb}} \quad (55)$$

$$\text{subject to } \sum_{k=1}^K \|\mathbf{f}_k\|^2 = 1. \quad (56)$$

Next, we put forth how to apply the proposed GPI-HIA method to solve (55).

B. Generalized Power Iteration for Downlink NOMA

We follow the same step with the proposed GPI-HIA. We first rewrite (54) by representing the precoding vectors onto the higher dimensional space as in (16):

$$R_{i,k}^{\text{lb}} = \log_2 \left(\frac{\bar{\mathbf{f}}^H \hat{\mathbf{A}}_{i,k} \bar{\mathbf{f}}}{\bar{\mathbf{f}}^H \hat{\mathbf{B}}_{i,k} \bar{\mathbf{f}}} \right), \quad (57)$$

where

$$\hat{\mathbf{A}}_{i,k} = \text{blkdiag} \left(\mathbf{0}, \dots, \mathbf{0}, \underbrace{\hat{\mathbf{h}}_i \hat{\mathbf{h}}_i^H + \Phi_i}_{k\text{th block}}, \dots, \hat{\mathbf{h}}_i \hat{\mathbf{h}}_i^H + \Phi_i \right) + \frac{\sigma^2}{P} \mathbf{I}_{NK} \in \mathbb{C}^{NK \times NK}, \quad (58)$$

$$\hat{\mathbf{B}}_{i,k} = \hat{\mathbf{A}}_{i,k} - \text{blkdiag} \left(\mathbf{0}, \dots, \mathbf{0}, \underbrace{\hat{\mathbf{h}}_i \hat{\mathbf{h}}_i^H}_{k\text{th block}}, \mathbf{0}, \dots, \mathbf{0} \right) \in \mathbb{C}^{NK \times NK}. \quad (59)$$

Subsequently, we approximate the minimum function included in the optimization problem by leveraging (57) and the LogSumExp technique:

$$\min_{i \geq k} \{R_{i,k}^{\text{lb}}\} \approx -\frac{1}{\alpha} \log \left(\sum_{i=k}^K e^{-\alpha R_{i,k}^{\text{lb}}} \right) = -\frac{1}{\alpha} \log \left(\sum_{i=k}^K \left(\frac{\bar{\mathbf{f}}^H \hat{\mathbf{A}}_{i,k} \bar{\mathbf{f}}}{\bar{\mathbf{f}}^H \hat{\mathbf{B}}_{i,k} \bar{\mathbf{f}}} \right)^{-\beta} \right), \quad (60)$$

where $\beta = \alpha \frac{1}{\log 2}$. Finally, the problem (55) is reformulated as

$$\max_{\bar{\mathbf{f}}} \sum_{k=1}^K -\frac{1}{\alpha} \log \left(\sum_{i=k}^K \left(\frac{\bar{\mathbf{f}}^H \hat{\mathbf{A}}_{i,k} \bar{\mathbf{f}}}{\bar{\mathbf{f}}^H \hat{\mathbf{B}}_{i,k} \bar{\mathbf{f}}} \right)^{-\beta} \right). \quad (61)$$

To obtain a solution of (61), we drive a first-order KKT condition in the following corollary.

Corollary 2. *The first-order KKT condition of the optimization problem (61) is satisfied if the following holds.*

$$\mathbf{B}_{\text{NOMA}}^{-1}(\bar{\mathbf{f}})\mathbf{A}_{\text{NOMA}}(\bar{\mathbf{f}}) = \lambda_{\text{NOMA}}(\bar{\mathbf{f}})\bar{\mathbf{f}} \quad (62)$$

where

$$\mathbf{A}_{\text{NOMA}}(\bar{\mathbf{f}}) = \lambda_{\text{NOMA}}^{(\text{num})}(\bar{\mathbf{f}}) \times \sum_{k=1}^K \left(\sum_{i=k}^K \beta \left(\frac{\bar{\mathbf{f}}^H \hat{\mathbf{A}}_{i,k} \bar{\mathbf{f}}}{\bar{\mathbf{f}}^H \hat{\mathbf{B}}_{i,k} \bar{\mathbf{f}}} \right)^{-\beta} \frac{\hat{\mathbf{A}}_{i,k}}{\bar{\mathbf{f}}^H \hat{\mathbf{A}}_{i,k} \bar{\mathbf{f}}} \right) / \sum_{i=k}^K \left(\frac{\bar{\mathbf{f}}^H \hat{\mathbf{A}}_{i,k} \bar{\mathbf{f}}}{\bar{\mathbf{f}}^H \hat{\mathbf{B}}_{i,k} \bar{\mathbf{f}}} \right)^{-\beta}, \quad (63)$$

$$\mathbf{B}_{\text{NOMA}}(\bar{\mathbf{f}}) = \lambda_{\text{NOMA}}^{(\text{den})}(\bar{\mathbf{f}}) \times \sum_{k=1}^K \left(\sum_{i=k}^K \beta \left(\frac{\bar{\mathbf{f}}^H \hat{\mathbf{A}}_{i,k} \bar{\mathbf{f}}}{\bar{\mathbf{f}}^H \hat{\mathbf{B}}_{i,k} \bar{\mathbf{f}}} \right)^{-\beta} \frac{\hat{\mathbf{B}}_{i,k}}{\bar{\mathbf{f}}^H \hat{\mathbf{B}}_{i,k} \bar{\mathbf{f}}} \right) / \sum_{i=k}^K \left(\frac{\bar{\mathbf{f}}^H \hat{\mathbf{A}}_{i,k} \bar{\mathbf{f}}}{\bar{\mathbf{f}}^H \hat{\mathbf{B}}_{i,k} \bar{\mathbf{f}}} \right)^{-\beta}, \quad (64)$$

with

$$\lambda_{\text{NOMA}} = \sum_{k=1}^K -\frac{1}{\alpha} \log \left(\sum_{i=k}^K \left(\frac{\bar{\mathbf{f}}^H \hat{\mathbf{A}}_{i,k} \bar{\mathbf{f}}}{\bar{\mathbf{f}}^H \hat{\mathbf{B}}_{i,k} \bar{\mathbf{f}}} \right)^{-\beta} \right) = \frac{\lambda_{\text{NOMA}}^{(\text{num})}(\bar{\mathbf{f}})}{\lambda_{\text{NOMA}}^{(\text{den})}(\bar{\mathbf{f}})}. \quad (65)$$

Proof. The proof is straightforward by removing the secrecy condition to the partial derivative of $\lambda_{\text{nc}}(\bar{\mathbf{f}})$ in Appendix A.1. \square

Now, to find the principal eigenvector of (62), we propose the GPI-NOMA algorithm.

$$\bar{\mathbf{f}}_{(t)} \leftarrow \frac{\mathbf{B}_{\text{NOMA}}^{-1}(\bar{\mathbf{f}}_{(t-1)})\mathbf{A}_{\text{NOMA}}(\bar{\mathbf{f}}_{(t-1)})\bar{\mathbf{f}}_{(t-1)}}{\left\| \mathbf{B}_{\text{NOMA}}^{-1}(\bar{\mathbf{f}}_{(t-1)})\mathbf{A}_{\text{NOMA}}(\bar{\mathbf{f}}_{(t-1)})\bar{\mathbf{f}}_{(t-1)} \right\|}. \quad (66)$$

We repeat this process until the convergence criterion is met. For the convergence condition, we use $\|\bar{\mathbf{f}}_{(t)} - \bar{\mathbf{f}}_{(t-1)}\| < \epsilon$, where ϵ is the predetermined tolerance level.

VI. NUMERICAL RESULTS

In this section, we evaluate the ergodic sum secrecy spectral efficiency to validate the performance of the proposed GPI-HIA. For comparison, we consider the following baseline methods:

- **Maximum ratio transmission (MRT):** since we assume a multigroup multicast scenario, it is not feasible to compute a precoding vector in a straightforward way. To obtain the precoding vectors, we construct $\mathbf{h}_k = \sum_{i \in \mathcal{L}_k} \mathbf{h}_{i,k}$ and use \mathbf{h}_k as an effective channel vector for the users in \mathcal{L}_k . With this, the precoding vectors are designed by matching the effective channel, i.e., $\mathbf{f}_k = \mathbf{h}_k$.
- **Zero-forcing (ZF):** we also use the effective channel vectors defined above. The precoding vectors are designed by following ZF methods as $\mathbf{F} = \mathbf{H} \left(\mathbf{H}^H \mathbf{H} \right)^{-1}$, where $\mathbf{F} = [\mathbf{f}_1, \dots, \mathbf{f}_K]$ and $\mathbf{H} = [\mathbf{h}_1, \dots, \mathbf{h}_K]$.

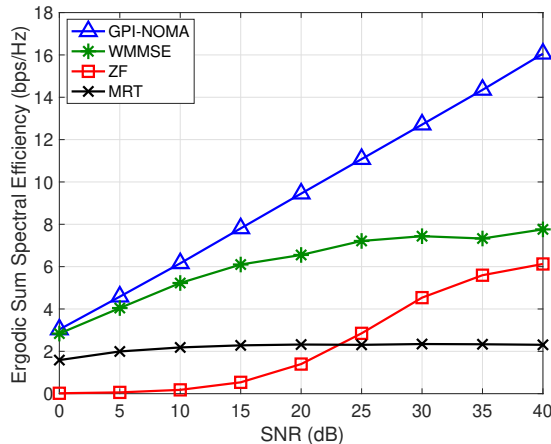


Fig. 2. Ergodic sum spectral efficiency in downlink NOMA system when SNR is increasing. The simulation parameters are $N = 4$, $K = 8$, $\kappa = 0.4$, $|\mathcal{L}_k| = 1$, $\epsilon = 0.01$, $\Delta_k = \pi/6$ for $k \in \{1, \dots, K\}$, and $\theta_k = \frac{\pi}{6}$.

- Multicast weighted minimum mean square error (WMMSE): in this method, the conventional WMMSE precoding [34] is modified for a multi-group multicast scenario [35]. Specifically, using the correspondence between mutual information and MMSE, a WMSE minimization problem was formulated. To release the non-convexity of the problem, the original problem was reformulated to a smooth constrained optimization problem with auxiliary variables. To solve this reformulated problem, the exponential penalty method was adopted. We note that this method finds a local optimal point of a general multi-group multicast scenario, while it does not incorporate our HIA condition.

In the proposed GPI-HIA setting, the LogSumExp approximation parameter α is determined as follows: we initialize it as $\alpha_1 = 10$ and if the proposed algorithm does not converge within a certain number of iterations $T = 50$, updating it as $\alpha_{n+1} = 0.9\alpha_n$.

A. Downlink MISO NOMA

At first, we illustrate the comparison of the ergodic sum spectral efficiency for the downlink MU-MISO system in Fig. 2 when the signal-to-noise ratio (SNR) is increasing. As baseline methods, we use the conventional precoding methods: 1) MRT, 2) ZF, and 3) WMMSE. Note that the WMMSE method in the downlink NOMA case is a reduced version of the multicast WMMSE [35] by assuming that each layer has only one user. We assume that all the users are clustered in a specific location.

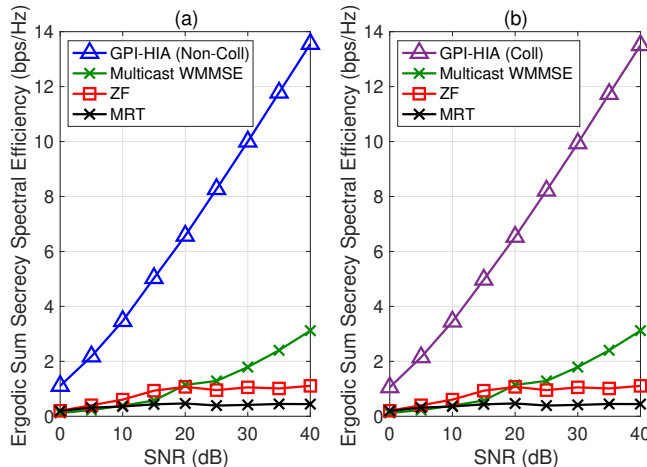


Fig. 3. Ergodic sum secrecy rate with (a) non-colluding case and (b) colluding case when SNR is increasing. The simulation parameters are $N = 6$, $K = 3$, $|\mathcal{L}_k| = 2$, $\epsilon = 0.01$, $\beta_m = 1$, $\Delta_m = \pi/6$ for $m \in \mathcal{M}$, and $\theta_m = [0, 2\pi]$.

We observe that the proposed algorithm outperforms the baseline methods in all the SNR regimes. Specifically, when the SNR is 40 dB, it shows about 200% gains over the WMMSE precoding method. This is because the proposed algorithm is designed by incorporating imperfect CSIT.

B. Secrecy Rate Comparison per SNR

In this subsection, we illustrate the comparison for the ergodic sum secrecy spectral efficiency per SNR in Fig. 3. Fig. 3(a) shows the performance comparison in the non-colluding case and Fig. 3(b) shows the performance comparison in the colluding case. In the both case, the proposed algorithm provides the highest performance compared to the baseline method. The noticeable point is that more gains are achieved in the high SNR regime. Especially, when the transmit SNR is 40dB, the proposed GPI-HIA provides about 460% gains over WMMSE. This is because the GPI-HIA is designed by properly incorporating the intertwined HIA condition. If the HIA condition is not reflected into the algorithm, the degrees-of-freedom of the sum secrecy spectral efficiency is degraded as observed in Fig. 3.

C. Secrecy Rate Comparison per the Number of the Users

In this subsection, we illustrate the simulation results in Fig. 4 when the number of users increases. Fig. 4(a) shows the performance comparison in the non-colluding case and Fig. 4(b)

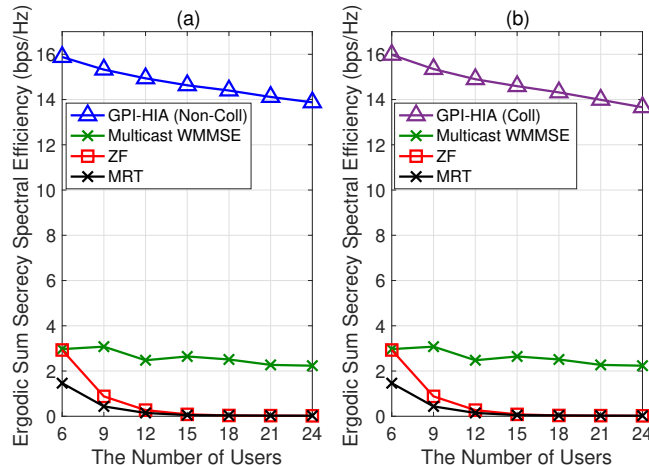


Fig. 4. Ergodic sum secrecy rate when the number of users is increasing in (a) non-colluding case and (b) colluding case. The simulation parameters are $N = 24$, $K = 3$, $|\mathcal{L}_k| = \frac{|\mathcal{M}|}{K}$, $\epsilon = 0.01$, $\text{SNR} = 40\text{dB}$, $\beta_m = 1$, $\Delta_m = \pi/6$ for $m \in \mathcal{M}$, and $\theta_m = [0, 2\pi]$.

shows the performance comparison in the colluding case. Since a multi-group multicast message scenario is considered, it is natural that the sum secrecy spectral efficiency decreases as the number of users increases. In Fig. 4, ZF and MRT achieve almost 0 sum secrecy spectral efficiency if the number of users is larger than 15. On contrary to that, the proposed GPI-HIA gets robust sum secrecy spectral efficiency compared to baseline methods.

D. Convergence

Fig. 5 shows the convergence results in terms of $\lambda_{nc}(\bar{\mathbf{f}})$, $\lambda_c(\bar{\mathbf{f}})$ and residual $\|\bar{\mathbf{f}}_{(t)} - \bar{\mathbf{f}}_{(t-1)}\|$ during 50 iterations. It is observed that both GPI-HIA (Non-Coll) and GPI-HIA (Coll) converge within 10 iterations. This provides an empirical evidence that the proposed GPI-HIA reaches a desirable local optimal point fast.

E. Fairness

In this subsection, we draw system level simulation results for resolving the fairness issue by incorporating the PF policy in the GPI-HIA. For a large scale fading parameter β_m used in system level simulation, we adopt the log-distance pathloss model in [36]. The distance between the BS and the users is 100m to 500m. We consider a 2.4 GHz carrier frequency with 10MHz bandwidth, -174 dBm/Hz noise power spectral density, and 9 dB noise figure.

The empirical cumulative distribution function (CDF) for the secrecy rate is depicted in Fig. 6(a). The GPI-HIA-PF shows a steeper curve than the GPI-HIA, i.e., the proposed algorithm

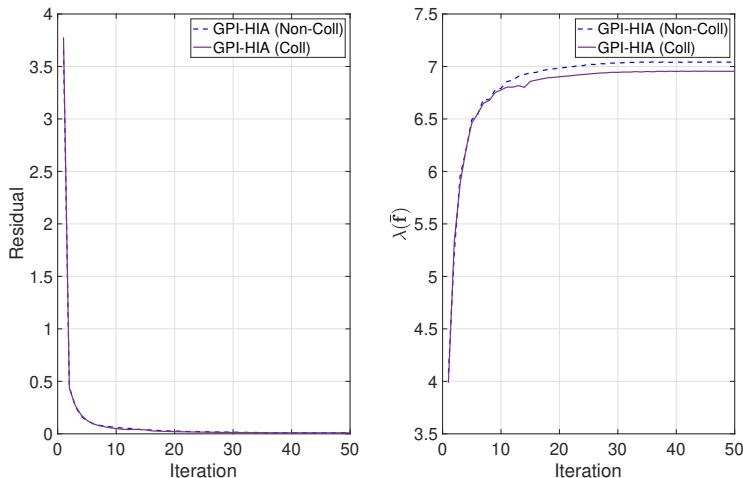


Fig. 5. Convergence results in terms of $\lambda(\hat{\mathbf{f}})$ and the residual $\|\hat{\mathbf{f}}_{(t)} - \hat{\mathbf{f}}_{(t-1)}\|$. The simulation parameters are $N = 6$, $K = 3$, $|\mathcal{L}_1| = 3$, $|\mathcal{L}_2| = 2$, $|\mathcal{L}_3| = 1$, $\epsilon = 0.01$, $\text{SNR} = 20\text{dB}$, $\Delta_m = \pi/6$ for $m \in \mathcal{M}$, $\theta_m = [0, 2\pi]$ and $\beta_m = 1$.

with PF policy provides more uniform secrecy rate to the users by resolving the fairness issue. For better understanding, we also present a snapshot of the achieved secrecy spectral efficiency for each layer in Fig. 6(b) and Fig. 6(c).

1) *Non-Colluding Case*: as the blue bar in the Fig. 6(b) shows, the power is concentrated on the message s_1 intended to the lowest layer users. After applying the PF policy to the GPI-HIA, the yellow bar in the Fig. 6(b), the secrecy rate for the messages intended to the higher layer increases.

2) *Colluding Case*: as the purple bar in Fig. 6(c) shows, we confirm that the power is concentrated on the message intended to the lower layer users. After applying the PF policy to the GPI-HIA, the green bar in Fig. 6(c), the secrecy rate for the messages intended to the higher layer increases.

VII. CONCLUSION

In this paper, we have considered a new security model that generalizes conventional physical layer security, referred to as HIA. Although the HIA is useful to reflect a hierarchical security structure, optimizing such a system is highly challenging due to its intertwined rate formations. Resolving the challenges, we have proposed new precoding methods to maximize the sum secrecy rate by considering the non-colluding and the colluding cases. Specifically, we have approximated non-smooth functions by using the LogSumExp technique and have reformulated

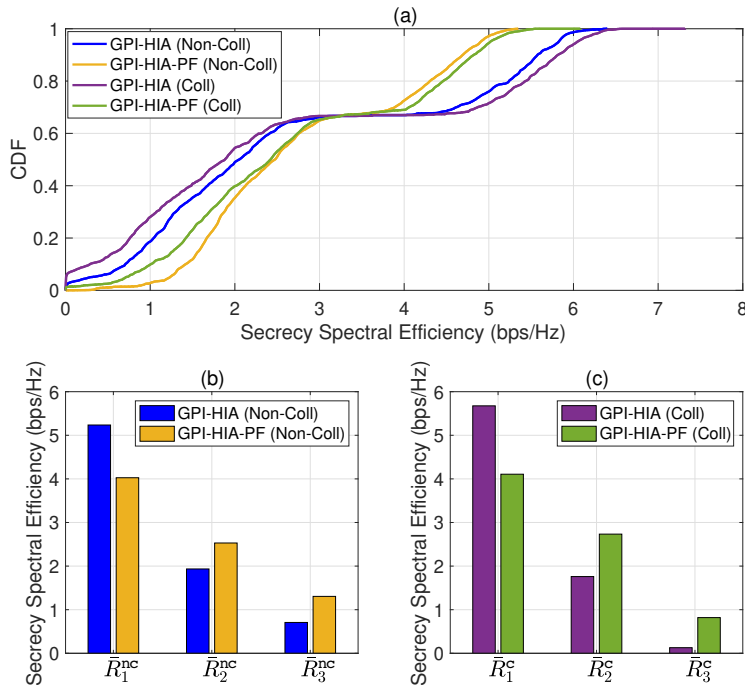


Fig. 6. Secrecy rate of each message in (a) non-colluding case and (b) colluding case. The simulation parameters are $N = 6$, $K = 3$, $|\mathcal{L}_1| = 3$, $|\mathcal{L}_2| = 2$, $|\mathcal{L}_3| = 1$, $\epsilon = 0.01$, $\delta = 0.2$, $\text{SNR} = 20\text{dB}$, $\Delta_m = \pi/6$ for $m \in \mathcal{M}$ and $\theta_m = [0, 2\pi]$.

the optimization problem as a form of Rayleigh quotients with a higher dimensional vector. With this form, we have derived the first-order optimality condition and cast this condition into a NEPv in which our objective function and precoding vector are mapped to the eigenvalue and eigenvector, respectively. Accordingly, our proposed methods compute the principal eigenvector to obtain a local optimal solution. As a byproduct, we have shown that the proposed precoding framework is also applicable to a sum rate maximization algorithm for downlink NOMA systems because the presented HIA model includes downlink NOMA with a fixed decoding order as a special case. Simulation results have validated that our methods provide significant performance improvement over existing baseline methods. In addition to this, our methods are beneficial in an implementation perspective since no off-the-shelf solver is used.

APPENDIX A.1

PROOF OF LEMMA 1

We first derive first-order KKT condition, i.e., $\frac{\partial \lambda_{\text{nc}}(\bar{\mathbf{f}})}{\partial \bar{\mathbf{f}}^{\text{H}}} = 0$ of the problem (23) where

$$\lambda_{\text{nc}}(\bar{\mathbf{f}}) = \sum_{k=1}^K \left(-\frac{1}{\alpha} \log \left(\sum_{\ell=k}^K \sum_{i \in \mathcal{L}_{\ell}} \left(\frac{\bar{\mathbf{f}}^{\text{H}} \mathbf{A}_{k,i,\ell} \bar{\mathbf{f}}}{\bar{\mathbf{f}}^{\text{H}} \mathbf{B}_{k,i,\ell} \bar{\mathbf{f}}} \right)^{-\beta} \right) - \frac{1}{\alpha} \log \left(\sum_{\ell'=1}^{k-1} \sum_{i' \in \mathcal{L}_{\ell'}} \left(\frac{\bar{\mathbf{f}}^{\text{H}} \mathbf{A}_{k,i',\ell'} \bar{\mathbf{f}}}{\bar{\mathbf{f}}^{\text{H}} \mathbf{B}_{k,i',\ell'} \bar{\mathbf{f}}} \right)^{\beta} \right) \right). \quad (67)$$

Using the derivative property, the partial derivative of $\lambda_{\text{nc}}(\bar{\mathbf{f}})$ is obtained as

$$\frac{\partial \lambda_{\text{nc}}(\bar{\mathbf{f}})}{\partial \bar{\mathbf{f}}^{\text{H}}} = -\frac{1}{\alpha} \sum_{k=1}^K \left(\frac{\sum_{\ell=k}^K \sum_{i \in \mathcal{L}_{\ell}} \left(-\beta \left(\frac{\bar{\mathbf{f}}^{\text{H}} \mathbf{A}_{k,i,\ell} \bar{\mathbf{f}}}{\bar{\mathbf{f}}^{\text{H}} \mathbf{B}_{k,i,\ell} \bar{\mathbf{f}}} \right)^{-\beta} \left(\frac{\mathbf{A}_{k,i,\ell} \bar{\mathbf{f}}}{\bar{\mathbf{f}}^{\text{H}} \mathbf{A}_{k,i,\ell} \bar{\mathbf{f}}} - \frac{\mathbf{B}_{k,i,\ell} \bar{\mathbf{f}}}{\bar{\mathbf{f}}^{\text{H}} \mathbf{B}_{k,i,\ell} \bar{\mathbf{f}}} \right) \right)}{\sum_{\ell=k}^K \sum_{i \in \mathcal{L}_{\ell}} \left(\frac{\bar{\mathbf{f}}^{\text{H}} \mathbf{A}_{k,i,\ell} \bar{\mathbf{f}}}{\bar{\mathbf{f}}^{\text{H}} \mathbf{B}_{k,i,\ell} \bar{\mathbf{f}}} \right)^{-\beta}} - \frac{\sum_{\ell'=1}^{k-1} \sum_{i' \in \mathcal{L}_{\ell'}} \left(\beta \left(\frac{\bar{\mathbf{f}}^{\text{H}} \mathbf{A}_{k,i',\ell'} \bar{\mathbf{f}}}{\bar{\mathbf{f}}^{\text{H}} \mathbf{B}_{k,i',\ell'} \bar{\mathbf{f}}} \right)^{\beta} \left(\frac{\mathbf{A}_{k,i',\ell'} \bar{\mathbf{f}}}{\bar{\mathbf{f}}^{\text{H}} \mathbf{A}_{k,i',\ell'} \bar{\mathbf{f}}} - \frac{\mathbf{B}_{k,i',\ell'} \bar{\mathbf{f}}}{\bar{\mathbf{f}}^{\text{H}} \mathbf{B}_{k,i',\ell'} \bar{\mathbf{f}}} \right) \right)}{\sum_{\ell'=1}^{k-1} \sum_{i' \in \mathcal{L}_{\ell'}} \left(\frac{\bar{\mathbf{f}}^{\text{H}} \mathbf{A}_{k,i',\ell'} \bar{\mathbf{f}}}{\bar{\mathbf{f}}^{\text{H}} \mathbf{B}_{k,i',\ell'} \bar{\mathbf{f}}} \right)^{\beta}} \right). \quad (68)$$

The first-order KKT condition holds when (68) equals to 0. Defining $\mathbf{A}_{\text{nc}}(\bar{\mathbf{f}})$, $\mathbf{B}_{\text{nc}}(\bar{\mathbf{f}})$ and $\lambda_{\text{nc}}(\bar{\mathbf{f}})$ as (25), (26) and (27), the first-order KKT condition is rearranged as

$$\mathbf{A}_{\text{nc}}(\bar{\mathbf{f}}) \bar{\mathbf{f}} = \lambda_{\text{nc}}(\bar{\mathbf{f}}) \mathbf{B}_{\text{nc}}(\bar{\mathbf{f}}) \bar{\mathbf{f}} \Leftrightarrow \mathbf{B}_{\text{nc}}^{-1}(\bar{\mathbf{f}}) \mathbf{A}_{\text{nc}}(\bar{\mathbf{f}}) \bar{\mathbf{f}} = \lambda_{\text{nc}}(\bar{\mathbf{f}}) \bar{\mathbf{f}}. \quad (69)$$

This completes the proof. \square

APPENDIX A.2

PROOF OF LEMMA 1

We first derive first-order KKT condition, i.e., $\frac{\partial \lambda_{\text{c}}(\bar{\mathbf{f}})}{\partial \bar{\mathbf{f}}^{\text{H}}} = 0$ of the problem (42) where

$$\lambda_{\text{c}}(\bar{\mathbf{f}}) = \sum_{k=1}^K \left(-\frac{1}{\alpha} \log \left(\sum_{\ell=k}^K \sum_{i \in \mathcal{L}_{\ell}} \left(\frac{\bar{\mathbf{f}}^{\text{H}} \mathbf{A}_{k,i,\ell} \bar{\mathbf{f}}}{\bar{\mathbf{f}}^{\text{H}} \mathbf{B}_{k,i,\ell} \bar{\mathbf{f}}} \right)^{-\beta} \right) - \frac{1}{\log 2} \log \left(\sum_{\ell'=1}^{k-1} \sum_{i' \in \mathcal{L}_{\ell'}} \left(\frac{\bar{\mathbf{f}}^{\text{H}} \mathbf{C}_{k,i',\ell'} \bar{\mathbf{f}}}{\bar{\mathbf{f}}^{\text{H}} \mathbf{D}_{k,i',\ell'} \bar{\mathbf{f}}} \right) \right) \right). \quad (70)$$

Using the similar technique in Lemma 1, the partial derivative of $\lambda_{\text{c}}(\bar{\mathbf{f}})$ is obtained by using the above calculation as

$$\frac{\partial \lambda_{\text{c}}(\bar{\mathbf{f}})}{\partial \bar{\mathbf{f}}^{\text{H}}} = \sum_{k=1}^K \left(-\frac{1}{\alpha} \frac{\sum_{\ell=k}^K \sum_{i \in \mathcal{L}_{\ell}} \left(-\beta \left(\frac{\bar{\mathbf{f}}^{\text{H}} \mathbf{A}_{k,i,\ell} \bar{\mathbf{f}}}{\bar{\mathbf{f}}^{\text{H}} \mathbf{B}_{k,i,\ell} \bar{\mathbf{f}}} \right)^{-\beta} \left(\frac{\mathbf{A}_{k,i,\ell} \bar{\mathbf{f}}}{\bar{\mathbf{f}}^{\text{H}} \mathbf{A}_{k,i,\ell} \bar{\mathbf{f}}} - \frac{\mathbf{B}_{k,i,\ell} \bar{\mathbf{f}}}{\bar{\mathbf{f}}^{\text{H}} \mathbf{B}_{k,i,\ell} \bar{\mathbf{f}}} \right) \right)}{\sum_{\ell=k}^K \sum_{i \in \mathcal{L}_{\ell}} \left(\frac{\bar{\mathbf{f}}^{\text{H}} \mathbf{A}_{k,i,\ell} \bar{\mathbf{f}}}{\bar{\mathbf{f}}^{\text{H}} \mathbf{B}_{k,i,\ell} \bar{\mathbf{f}}} \right)^{-\beta}} - \frac{1}{\log 2} \frac{\sum_{\ell'=1}^{k-1} \sum_{i' \in \mathcal{L}_{\ell'}} \frac{\bar{\mathbf{f}}^{\text{H}} \mathbf{C}_{k,i',\ell'} \bar{\mathbf{f}}}{\bar{\mathbf{f}}^{\text{H}} \mathbf{D}_{k,i',\ell'} \bar{\mathbf{f}}} \left(\frac{\mathbf{C}_{k,i',\ell'} \bar{\mathbf{f}}}{\bar{\mathbf{f}}^{\text{H}} \mathbf{C}_{k,i',\ell'} \bar{\mathbf{f}}} - \frac{\mathbf{D}_{k,i',\ell'} \bar{\mathbf{f}}}{\bar{\mathbf{f}}^{\text{H}} \mathbf{D}_{k,i',\ell'} \bar{\mathbf{f}}} \right)}{\sum_{\ell'=1}^{k-1} \sum_{i' \in \mathcal{L}_{\ell'}} \frac{\bar{\mathbf{f}}^{\text{H}} \mathbf{C}_{k,i',\ell'} \bar{\mathbf{f}}}{\bar{\mathbf{f}}^{\text{H}} \mathbf{D}_{k,i',\ell'} \bar{\mathbf{f}}}} \right). \quad (71)$$

The first-order KKT condition holds when (71) equals to 0. Defining $\mathbf{A}_c(\bar{\mathbf{f}})$, $\mathbf{B}_c(\bar{\mathbf{f}})$ and $\lambda_c(\bar{\mathbf{f}})$ as (44), (45) and (46), the first-order KKT condition is rearranged as

$$\mathbf{A}_c(\bar{\mathbf{f}})\bar{\mathbf{f}} = \lambda_c(\bar{\mathbf{f}})\mathbf{B}_c(\bar{\mathbf{f}})\bar{\mathbf{f}} \Leftrightarrow \mathbf{B}_c^{-1}(\bar{\mathbf{f}})\mathbf{A}_c(\bar{\mathbf{f}})\bar{\mathbf{f}} = \lambda_c(\bar{\mathbf{f}})\bar{\mathbf{f}}. \quad (72)$$

This completes the proof. □

REFERENCES

- [1] K. Lee, J. Choi, D. Kim, and J. Park, "Hierarchical information accessibility in downlink MIMO systems," *to appear in IEEE Glob. Commun. Conf.*, 2021.
- [2] J. L. Massey, "An introduction to contemporary cryptology," *Proceedings of the IEEE*, vol. 76, no. 5, pp. 533–549, May 1988.
- [3] A. D. Wyner, "The wire-tap channel," *The Bell System Technical Journal*, vol. 54, no. 8, pp. 1355–1387, Oct. 1975.
- [4] P. Porambage, G. Gür, D. P. M. Osorio, M. Liyanage, A. Gurtov, and M. Ylianttila, "The roadmap to 6G security and privacy," *IEEE Open J. of the Commun. Society*, vol. 2, pp. 1094–1122, 2021.
- [5] W. Zhang, J. Chen, Y. Kuo, and Y. Zhou, "Transmit beamforming for layered physical layer security," *IEEE Trans. Veh. Technol.*, vol. 68, no. 10, pp. 9747–9760, 2019.
- [6] M. Li, G. Ti, and Q. Liu, "Secure beamformer designs in MU-MIMO systems with multiuser interference exploitation," *IEEE Trans. Veh. Technol.*, vol. 67, no. 9, pp. 8288–8301, Sep. 2018.
- [7] P. Zhao, M. Zhang, H. Yu, H. Luo, and W. Chen, "Robust beamforming design for sum secrecy rate optimization in MU-MISO networks," *IEEE Trans. Info. Forensics and Security*, vol. 10, no. 9, pp. 1812–1823, Sep. 2015.
- [8] Z. Sheng, H. D. Tuan, T. Q. Duong, and H. V. Poor, "Beamforming optimization for physical layer security in MISO wireless networks," *IEEE Trans. Signal Process.*, vol. 66, no. 14, pp. 3710–3723, Jul. 2018.
- [9] J. Choi and J. Park, "SecureLinQ: Joint precoding and scheduling for secure device-to-device networks," *IEEE Wireless Commun. Lett.*, vol. 9, no. 12, pp. 2078–2082, 2020.
- [10] —, "Sum secrecy spectral efficiency maximization in downlink MU-MIMO: Colluding eavesdroppers," *IEEE Trans. Veh. Technol.*, vol. 70, no. 1, pp. 1051–1056, 2021.
- [11] N. Yang, P. L. Yeoh, M. Elkashlan, R. Schober, and I. B. Collings, "Transmit antenna selection for security enhancement in MIMO wiretap channels," *IEEE Trans. Commun.*, vol. 61, no. 1, pp. 144–154, Jan. 2013.
- [12] M. Yang, D. Guo, Y. Huang, T. Q. Duong, and B. Zhang, "Physical layer security with threshold-based multiuser scheduling in multi-antenna wireless networks," *IEEE Trans. Commun.*, vol. 64, no. 12, pp. 5189–5202, 2016.
- [13] Z. Ding, Z. Zhao, M. Peng, and H. V. Poor, "On the spectral efficiency and security enhancements of NOMA assisted multicast-unicast streaming," *IEEE Trans. Commun.*, vol. 65, no. 7, pp. 3151–3163, 2017.
- [14] Y. Li, M. Jiang, Q. Zhang, Q. Li, and J. Qin, "Secure beamforming in downlink MISO nonorthogonal multiple access systems," *IEEE Trans. Veh. Technol.*, vol. 66, no. 8, pp. 7563–7567, 2017.
- [15] G. W. Hsu, B. Liu, H. H. Wang, and H. J. Su, "Joint beamforming for multicell multigroup multicast with per-cell power constraints," *IEEE Trans. Veh. Technol.*, vol. 66, no. 5, pp. 4044–4058, 2017.
- [16] M. Sadeghi, E. Bjrnson, E. G. Larsson, C. Yuen, and T. Marzetta, "Joint unicast and multi-group multicast transmission in massive MIMO systems," *IEEE Trans. Wireless Commun.*, vol. 17, no. 10, pp. 6375–6388, 2018.
- [17] A. Adhikary, J. Nam, J. Ahn, and G. Caire, "Joint spatial division and multiplexing—the large-scale array regime," *IEEE Trans. Inf. Theory*, vol. 59, no. 10, pp. 6441–6463, 2013.

- [18] M. Dai, B. Clerckx, D. Gesbert, and G. Caire, "A rate splitting strategy for massive MIMO with imperfect CSIT," *IEEE Trans. Wireless Commun.*, vol. 15, no. 7, pp. 4611–4624, 2016.
- [19] F. Zhou, Z. Chu, H. Sun, R. Q. Hu, and L. Hanzo, "Artificial noise aided secure cognitive beamforming for cooperative MISO-NOMA using SWIPT," *IEEE J. Sel. Areas Commun.*, vol. 36, no. 4, pp. 918–931, 2018.
- [20] M. Tian, Q. Zhang, S. Zhao, Q. Li, and J. Qin, "Secrecy sum rate optimization for downlink MIMO nonorthogonal multiple access systems," *IEEE Signal Process. Lett.*, vol. 24, no. 8, pp. 1113–1117, 2017.
- [21] J. Kampeas, A. Cohen, and O. Gurewitz, "On secrecy rates and outage in multi-user multi-eavesdroppers MISO systems," in *Proc. IEEE Int. Symp. Info. Th.*, Jul. 2016, pp. 2449–2453.
- [22] Q. Li and W.-K. Ma, "Multicast secrecy rate maximization for MISO channels with multiple multi-antenna eavesdroppers," in *Proc. IEEE Int. Conf. on Comm.*, 2011, pp. 1–5.
- [23] J. Zhu, J. Wang, Y. Huang, K. Navaie, Z. Ding, and L. Yang, "On optimal beamforming design for downlink MISO NOMA systems," *IEEE Trans. Veh. Technol.*, vol. 69, no. 3, pp. 3008–3020, 2020.
- [24] C. Shen and H. Li, "On the dual formulation on boosting algorithms," *IEEE Trans. on Pattern Analysis and Machine Intelligence*, vol. 32, no. 12, pp. 2216–2231, 2010.
- [25] F. Nielsen and K. Sun, "Guaranteed bounds on information-theoretic measures of univariate mixtures using piecewise log-sum-exp inequalities," *SIAM Journal on Matrix Analysis and Applications*, vol. 18, no. 12, 2016.
- [26] Y. Cai, L. H. Zhang, Z. Bai, and R. C. Li, "On an eigenvector-dependent nonlinear eigenvalue problem," *SIAM Journal on Matrix Analysis and Applications*, vol. 39, no. 3, pp. 1360–1382, 2018.
- [27] J. Park, J. Choi, N. Lee, W. Shin, and H. V. Poor, "Rate-splitting multiple access for downlink MIMO: A generalized power iteration approach," *ArXiv Preprint*, 2021. [Online]. Available: <https://arxiv.org/abs/2108.06844>
- [28] J. Choi, J. Park, and N. Lee, "Energy efficiency maximization precoding for quantized massive MIMO systems," *ArXiv Preprint*, 2021. [Online]. Available: <https://arxiv.org/abs/2108.03048>
- [29] J. Choi, N. Lee, S. Hong, and G. Caire, "Joint user selection, power allocation, and precoding design with imperfect CSIT for multi-cell MU-MIMO downlink systems," *IEEE Trans. Wireless Commun.*, vol. 19, no. 1, pp. 162–176, Jan. 2020.
- [30] J. Krivochiza, J. Merlano Duncan, S. Andrenacci, S. Chatzinotas, and B. Ottersten, "FPGA acceleration for computationally efficient symbol-level precoding in multi-user multi-antenna communication systems," *IEEE Access*, vol. 7, pp. 15 509–15 520, 2019.
- [31] P. Viswanath, D. Tse, and R. Laroia, "Opportunistic beamforming using dumb antennas," *IEEE Trans. Inf. Theory*, vol. 48, no. 6, pp. 1277–1294, Jun. 2002.
- [32] J. Park, N. Lee, J. G. Andrews, and R. W. Heath, "On the optimal feedback rate in interference-limited multi-antenna cellular systems," *IEEE Trans. Wireless Commun.*, vol. 15, no. 8, pp. 5748–5762, 2016.
- [33] J. Park and R. W. Heath, "Multiple-antenna transmission with limited feedback in device-to-device networks," *IEEE Wireless Commun. Lett.*, vol. 5, no. 2, pp. 200–203, 2016.
- [34] S. S. Christensen, R. Agarwal, E. Carvalho, and J. M. Cioffi, "Weighted sum-rate maximization using weighted MMSE for MIMO-BC beamforming design," *IEEE Trans. Wireless Commun.*, vol. 7, no. 12, pp. 4792–4799, Dec. 2008.
- [35] A. Z. Yalcin and M. Yuksel, "Precoder design for multi-group multicasting with a common message," *IEEE Trans. Commun.*, vol. 67, no. 10, pp. 7302–7315, Oct. 2019.
- [36] V. Erceg, L. J. Greenstein, S. Y. Tjandra, S. R. Parkoff, A. Gupta, B. Kulic, A. A. Julius, and R. Bianchi, "An empirically based path loss model for wireless channels in suburban environments," *IEEE J. Sel. Areas Commun.*, vol. 17, no. 7, pp. 1205–1211, 1999.